PRIMARY RESEARCH ARTICLE

WILEY · Global Change Biology

Spatiotemporal remote sensing of ecosystem change and causation across Alaska

Neal J. Pastick[1,2] | M. Torre Jorgenson[3] | Scott J. Goetz[4] | Benjamin M. Jones[5] | Bruce K. Wylie[6] | Burke J. Minsley[7] | Hélène Genet[8] | Joseph F. Knight[2] | David K. Swanson[9] | Janet C. Jorgenson[10]

[1]Stinger Ghaffarian Technologies, Inc. (contractor to the U.S. Geological Survey), Sioux Falls, South Dakota

[2]Department of Forest Resources, University of Minnesota, St. Paul, Minnesota

[3]Alaska Ecoscience, Fairbanks, Alaska

[4]School of Informatics, Computing, and Cyber Systems, Northern Arizona University, Flagstaff, Arizona

[5]Alaska Science Center, U.S. Geological Survey, Anchorage, Alaska

[6]Earth Resources Observation and Science Center, U.S. Geological Survey, Sioux Falls, South Dakota

[7]Crustal Geophysics and Geochemistry Science Center, U.S. Geological Survey, Denver, Colorado

[8]Institute of Arctic Biology, University of Alaska Fairbanks, Fairbanks, Alaska

[9]National Park Service, Fairbanks, Alaska

[10]Arctic National Wildlife Refuge, U.S. Fish and Wildlife Service, Fairbanks, Alaska

Correspondence
Neal J. Pastick, Stinger Ghaffarian Technologies, Inc. (contractor to the U.S. Geological Survey), Sioux Falls, SD 57198.
Email: past0042@umn.edu

Abstract

Contemporary climate change in Alaska has resulted in amplified rates of press and pulse disturbances that drive ecosystem change with significant consequences for socio-environmental systems. Despite the vulnerability of Arctic and boreal landscapes to change, little has been done to characterize landscape change and associated drivers across northern high-latitude ecosystems. Here we characterize the historical sensitivity of Alaska's ecosystems to environmental change and anthropogenic disturbances using expert knowledge, remote sensing data, and spatiotemporal analyses and modeling. Time-series analysis of moderate—and high-resolution imagery was used to characterize land- and water-surface dynamics across Alaska. Some 430,000 interpretations of ecological and geomorphological change were made using historical air photos and satellite imagery, and corroborate land-surface greening, browning, and wetness/moisture trend parameters derived from peak-growing season Landsat imagery acquired from 1984 to 2015. The time series of change metrics, together with climatic data and maps of landscape characteristics, were incorporated into a modeling framework for mapping and understanding of drivers of change throughout Alaska. According to our analysis, approximately 13% (~174,000 $\pm$ 8700 km^2) of Alaska has experienced directional change in the last 32 years ($\pm$95% confidence intervals). At the ecoregions level, substantial increases in remotely sensed vegetation productivity were most pronounced in western and northern foothills of Alaska, which is explained by vegetation growth associated with increasing air temperatures. Significant browning trends were largely the result of recent wildfires in interior Alaska, but browning trends are also driven by increases in evaporative demand and surface-water gains that have predominately occurred over warming permafrost landscapes. Increased rates of photosynthetic activity are associated with stabilization and recovery processes following wildfire, timber harvesting, insect damage, thermokarst, glacial retreat, and lake infilling and drainage events. Our results fill a critical gap in the understanding of historical and potential future trajectories of change in northern high-latitude regions.

KEYWORDS
Arctic, boreal forest, coastal processes, glaciers, insect damage, shrub expansion, surface water, thermokarst, time-series analysis, wildfire

1 | INTRODUCTION

Arctic and boreal ecosystems have recently seen dramatic changes in vegetation characteristics (Beck & Goetz, 2011; Goetz, Bunn, Fiske, & Houghton, 2005; Ju & Masek, 2016; Myers-Smith et al., 2011), surface water area (Carroll, Townshend, DiMiceli, Loboda, & Sohlberg, 2011), and disturbance regimes, such as wildland fire (Kasischke et al., 2010), permafrost degradation (Jorgenson, Racine, Walters, & Osterkamp, 2001; Lara et al., 2016), and insect/disease infestation (Berg, Henry, Fastie, De Volder, & Matsuoka, 2006; Parent & Verbyla, 2010; Verbyla, 2011), that can have a substantial impact on socio-ecological systems (Chapin et al., 2006). Growth in high-latitude vegetation and disturbance regimes are widely expected to increase with rising atmospheric CO_2 and air temperature (Chapin et al., 2006; Genet et al., 2018; Pastick et al., 2017), which may trigger transitions in ecosystem trajectories that will affect biological and physical processes at a multitude of scales (Hinzman et al., 2013).

Earth observation satellite and suborbital data are invaluable for quantifying land- and water-surface dynamics across the globe (Hansen et al., 2013; Pekel, Cottam, Gorelick, & Belward, 2016). Recent studies have made use of dense time stacks of moderate resolution imagery to characterize trends in land-surface features throughout Arctic and boreal ecosystems of North America and Eurasia (Fraser, Olthof, Carrière, Deschamps, & Pouliot, 2011; Fraser et al., 2014; Hermosilla, Wulder, White, Coops, & Hobart, 2015; Ju & Masek, 2016; Nitze et al., 2017; Olthof & Fraser, 2014), but these studies did not focus on attribution of the drivers of observed changes manifested in these datasets at regional scales. Despite a legacy of studies documenting recent changes across northern ecosystems, a large challenge remains to quantify ecological change and associated drivers across heterogeneous high-latitude regions (Jorgenson, Marcot, Swanson, Jorgenson, & DeGange, 2015).

Here, we quantify contemporary landscape dynamics in Alaska related to environmental change and anthropogenic disturbances (e.g., road and infrastructure development, natural resource extraction and exploration) using manual-image interpretations and the historical (1984–2015) 30 m Landsat archive. Spectral change metrics, climatic data, topographical and soils information, and examples of change were used to develop statistical models for the prediction and understanding of drivers of change throughout Alaska. In so doing, we address the following questions: (1) How do environmental changes and anthropogenic disturbances manifest themselves within trends maps derived from Landsat imagery? (2) What is the spatial extent of changes that have occurred across the landscape in the last 32 years? (3) Which environmental factors (e.g., climate, biophysical) appear to be associated with land- and water-surface dynamics at the regional scale? (4) Based on observations of historic change in Alaska, which regions are most vulnerable to change during the 21st century? The results from this study fill a critical gap in understanding the historical—and potential future—face of Alaska.

2 | MATERIALS AND METHODS

2.1 | Spatiotemporal extent of the study

The study area included terrestrial and aquatic ecosystems (as defined by Nowacki, Spencer, Fleming, Brock, & Jorgenson, 2003) of Alaska, excluding the Alaskan Peninsula and Bering Sea Islands due to data constraints, totaling 1.4M km^2, or the equivalent of 1.6B 30 m Landsat pixels (Figure 1). For this study, change was defined as an alteration to surface conditions due to disturbance, or ecological or geomorphological processes (i.e., fluvial, coastal, and lacustrine dynamics, erosion and deposition, wildland fires, insect damage, succession, glacial retreat and expansion, shrub expansion, thermokarst, human impacts) at the Landsat pixel scale. Areas with no change are defined as the lack of alteration to surface features at the 30 m pixel scale.

The overall workflow for data processing and change modeling consisted of 10 steps, which can be assembled into three groups: (1) automated Landsat preprocessing; (2) trend analyses and geodatabase development; and; (3) classifier and map development. Automated Landsat preprocessing included: (1) image filtering; (2) conversion of raw digital values (DN) to top of atmosphere (TOA) reflectance; (3) cloud/shadow screening; (4) image stacking, and; (5) data normalization. Time-series analyses includes (1) manual image interpretation to assess change drivers, which made use of historical air photos and high-resolution satellite imagery (1980s, 1990s, 2000s, 2010s), and (2) linear regression models fit to Landsat imagery (i.e., Thematic Mapper [TM], Enhanced Thematic Mapper Plus [ETM+], and Operational Land Imager [OLI]) Level 1T) and (3) estimates of annual permanent surface water area derived from Landsat imagery (Pekel et al., 2016). A detailed description of each processing step, data layers, and analyses are discussed below.

2.2 | Landsat preprocessing, time-series analyses, and spectral change metrics

Landsat image processing and trend calculations were performed within Google's Earth Engine (GEE) JAVASCRIPT API (Gorelick et al., 2017). A Javascript program was developed within the GEE API to ingest and preprocess imagery, and for trend analyses of spectral indices derived from Landsat imagery. Landsat (i.e., Thematic Mapper [TM], Enhanced Thematic Mapper Plus [ETM+], and Operational Land Imager [OLI]) Level 1T) calibrated top-of-atmosphere (TOA) reflectance data was filtered using cloud cover metrics (less than 80%) and image acquisition dates (1984–2016) corresponding to summer (May 1st–September 30th) and peak-growing season months (July 1st–August 31st). Images acquired in the growing season were used as inputs into linear regression models because constraining the time range to peak greenness eliminates seasonal variations in reflectance values that increase errors associated with phenological phases between different ecozones. A statistical-transformation function was used to calibrate spectral indices (see descriptions below) derived from Landsat OLI data (Roy et al., 2016),
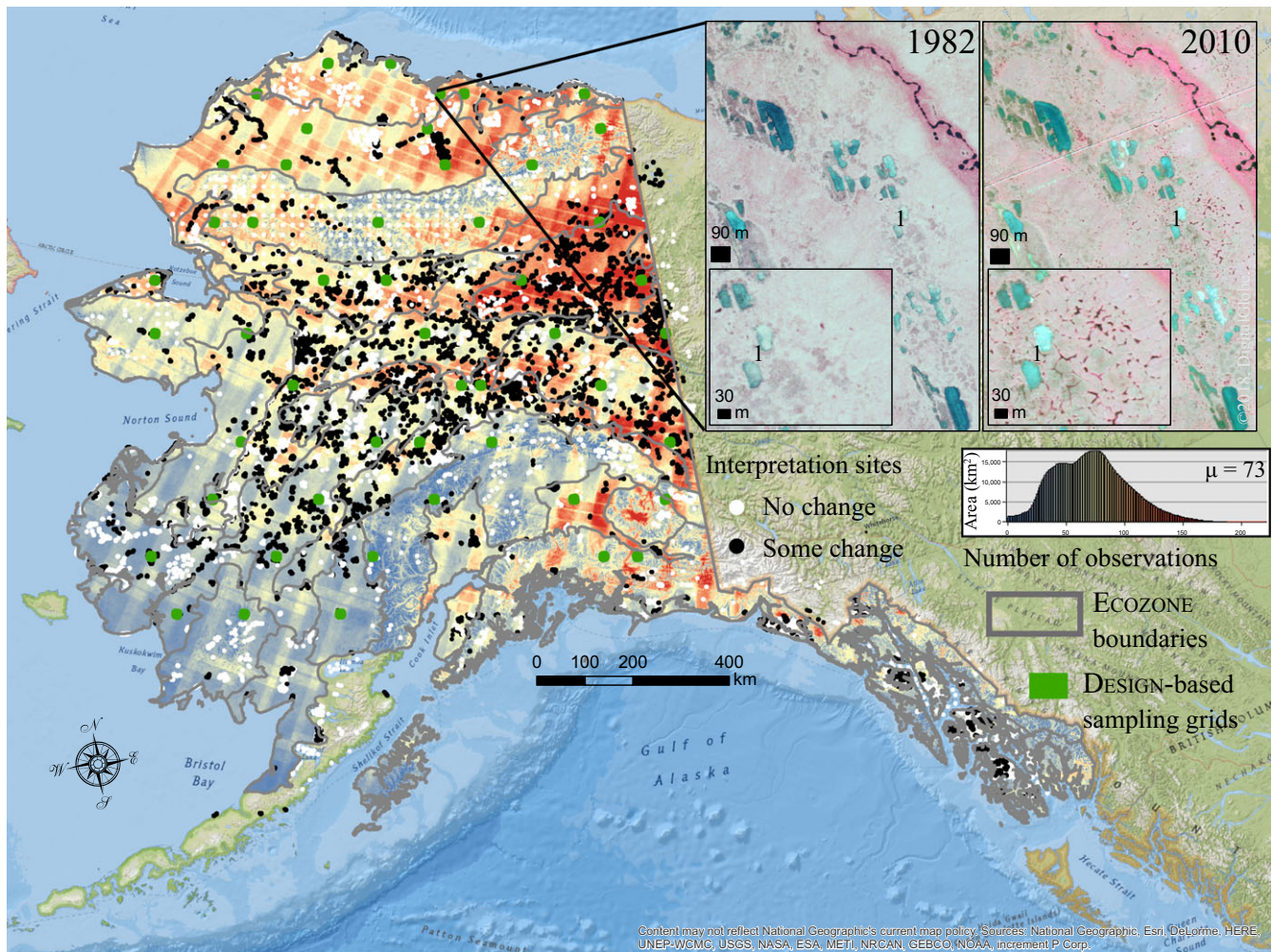
FIGURE 1 Interpretation sites, ecozone boundaries (Nowacki et al., 2003), and design-based sample grids draped over the number of valid Landsat observations (Thematic Mapper [TM], Enhance Thematic Mapper Plus [ETM+], Operational Land Imager [OLI]) from 1984 and 2015 in Alaska. Inset shows Alaska High Altitude Aerial Photograph (AHAP) and high-resolution imagery (copyright DigitalGlobe, Inc.) used to delineate change processes (e.g., thermokarst, infrastructure development) occurring across the landscape

to improve temporal continuity between other Landsat sensor data, although calculation of sensor-specific TOA reflectance values results in a highly normalized dataset with minor differences occurring due to slight differences in radiometric bandwidths of each sensor (Ju & Masek, 2016; Markham & Helder, 2012). Calibrated TOA reflectance data were used instead of surface reflectance (SR) data because of the lack of MODIS data needed to constrain atmospheric correction models for a portion of the time series (1984–2000) and known uncertainties associated with Landsat SR data over high latitudes (above 65°N).

A large number (n = 13,000–34,000) of Landsat scenes were available in our study area, using our filtering criteria, with the majority coming from 2000 to 2015 (Supporting Information Figure S1). The *FMask* algorithm (Zhu & Woodcock, 2014) was used to mask 30 m pixels identified to be clouds and shadows. Top-of-atmosphere reflectance values were transformed into Normalized Difference Vegetation Index (NDVI), Normalized Difference Infrared Index (NDII7), Normalized Difference Moisture Index (NDMI), Normalized

Difference Water Index (NDWI) spectral indices, for each unobstructed pixel, which serve as a proxy for vegetation productivity and status, surface moisture, and water content (Gao, 1996; Goetz & Prince, 1999; Ji et al., 2012). Because studies have shown that there is little difference between NDMI and NDWI values derived from different Landsat sensors (Holden & Woodcock, 2016), a statistical-calibration function was only used to correct for potential (but slight) biases in NDVI values calculated from Landsat OLI data.

Linear trends were calculated for each spectral index using nonparametric, Theil–Sen Regression (TSR) models within GEE. TSR was calculated for each 30 m pixel by determining the slope between every pairwise combination of images in time and then finding the median value. TSR is insensitive to outliers with a breakdown point of approximately 29% and, thus, can outperform ordinary least square regression analysis (Fernandes & Leblanc, 2005). The precision of the TSL parameters at any location improves as the number of valid observations increases. The heat map shown in Figure 1

documents the number of peak-growing season observations for each pixel location, which can serve a measure of confidence, although these numbers could be considered inflated where WRS-2 rows overlap.

Synthetic image stacks of late-season multispectral indices were generated from harmonic models that were fit to the filtered Landsat archive using a 3 year sliding window approach (2000–2015; January 1st–December 31st). Per-cell metrics (i.e., standard deviation, range) were generated from each image stack, for inclusion in the change detection model, to identify ephemeral disturbances (assuming that volatility is a proxy for change) that would not be captured using TSR. Multiyear, 90th percentile mosaics (1984–1999) were also generated from summer Landsat TM imagery, because of the dearth of imagery in the 80s and 90s, to help characterize changes that might have happened early in the study period.

The amount and direction of changes in annual permanent surface water area was quantified by performing linear regression analysis on estimates made by Pekel et al. (2016) from 1984 to 2015. Derived trend parameters (e.g., Pearson's r, slope, p-value) were computed using years where the unobserved area of the maximum water extent (any pixel that has ever been identified as permanent water across the study period) was less than 5%, because gaps in the observation record could result in underestimation of the reported areas. Linear regression analysis was conducted using a grid system (5 × 5 km), because the unobserved component of the maximum water extent is likely to be much greater when summarizing trends across large areas (e.g., ecozones), and trend parameters from each grid were summarized by ecozone. Note, that the solar illumination threshold (30°) used when developing the annual surface water layers (v1.0) results in a lower number of valid observations within higher latitude regions, particularly above 65°N.

2.3 | Drivers and attribution of change

2.3.1 | Interpretations of land-surface change

Photo-interpretation techniques were used to quantify ecological and geomorphic change drivers across 262 change grids (Jorgenson & Brown, 2015; Jorgenson et al., 2001, 2015; Swanson, 2013) using the system described in Jorgenson et al. (2015). Change grids were systematically or randomly distributed across the Arctic Network (ARCN) of national parks, Selawik National Wildlife Refuge, Arctic National Wildlife Refuge (ANWR), Tanana-Kuskokwim Lowlands, and Yukon-Tanana Uplands. At each grid, 2–4 high-resolution aerial and satellite images, from different times periods (1980s, 2000s, 2010s), were acquired and georectified using a publicly available statewide SPOT mosaic or IKONOS imagery. Approximately 40–100 locations were systematically sampled along each change grid for time-series analysis, for approximately 13,000 expert interpretations. Change drivers were assessed at the middle of each point location.

Historical (1984–2015) Landsat data and high-resolution imagery (i.e., Alaska High-Altitude Photography [AHAP], WorldView-2 and 3, GeoEye-1) were used to make additional interpretations

(n = 390,000) outside the extent of the change grids. Since collecting reliable interpretations is a costly and time-consuming task, easily acquired interpretations from other sources (e.g., Monitoring Trends and Burn Severity Data [MTBS]; Eidenshink et al., 2007) were also used (n = 25,000), which may be less reliable than expert interpretation. In total, approximately 430,000 interpretations were used to calibrate empirical models discussed in the predictive modeling and mapping portion of the paper. Note that manual interpretation of thermokarst occurrence in bedrock-controlled terrain, which covers approximately 30% of Alaska (Jorgenson et al., 2008), was not feasible in most instances because of the lack of a surface deformation from thawing permafrost in ice-poor soils.

2.3.2 | Attribution of spectral index changes

Trends in growing season remotely sensed vegetation productivity and wetness indices (i.e., Normalized Difference Vegetation Index, NDVI; Normalized Difference Water Index, NDWI) were analyzed with respect to ecological and geomorphological change (or no change), identified from time series of high-resolution imagery of surface water (Jones et al., 2011), coastal areas (Arp, Jones, Schmutz, Urban, & Jorgenson, 2010; Jones et al., 2009), thermokarst (Jones et al., 2016; Swanson, 2014), glacial areas (Loso, A. Arendt, & J. Rich, 2014), and geomorphic and vegetation change studies discussed in the previous section. Student's t tests and Wilcoxon—Mann–Whitney U-tests were used to test the significance of differences in mean trend values between sample locations of change and no change. Diagnostic plots were used to assess normality and homoscedasticity.

To evaluate the relative impacts of wildfires, insects, and timber harvesting and subsequent recovery of vegetation, we employed a space-for-time design (Pickett, 1989), where slope values (i.e., NDVI/year) were averaged within disturbance perimeters, and the relationship between time since disturbance and changes in late-season vegetation productivity were assessed using Generalized Additive Models (GAM; Wood, 2006). The main assumption of this method is that observing locations of varying time since disturbance would produce similar results to observing locations through time. To generate our chronosequence, we used historical fire (1940–2015), insect damage (1997–2015), and timber harvest (1950–2015) perimeter data, as obtained from the Bureau of Land Management (http://www.fire.ak.blm.gov) and the United States Forest Service (http://foresthealth.fs.usda.gov; https://catalog.data.gov/dataset/u-s-forest-service-timber-harvests). We excluded areas identified to have been impacted by multiple disturbances (i.e., repeatedly burned, insect damage and harvested) and sampled the remaining locations within the perimeters. Note, that we assumed that the survey years reported in the insect/disease datasets were fair approximations for the timing of disturbance, as this information was not available, and acknowledge that disturbances may not have impacted all areas within the disturbance perimeters. Selection of the best-fit models to describe the studied relationships were based on Akaike's Information Criteria (AIC) and Generalized Cross

Validation (GCV) scores derived from a leave-one-out cross valida-tion estimation process. Model residuals were inspected to ensure that selection of the best-fit model was not adversely impacted by outliers and noise. Residual error was modeled using a first order autoregressive (AR1) model to explicitly account for temporal auto-correlation in trend values, where appropriate. GAM models were developed using the *mgcv* package in R (https://cran.r-project.org/web/packages/mgcv/), with a cubic regression spline, which are well suited to depict nonlinear trends associated with stand age and veg-etation productivity.

2.4 | Regional analysis of vegetation and surface-water dynamics

Regional controllers of vegetation productivity and surface-water dynamics were assessed using a spatial framework of ecozone boundaries (Nowacki et al., 2003; Figure 1). The effect of climatic indices, topographic information, modeled permafrost presence/ab-sence data, and mapped soil texture extents were evaluated using regression models.

Climate variables representing energy and demand were con-structed from monthly mean temperature, air vapor pressure, and total precipitation data from the climate research unit (CRU; Harris, Jones, Osborn, & Lister, 2014). Historical CRU TS 4.0 data were sta-tistically downscaled via the delta method (Hayhoe, VanDorn, Croley, Schlegal, & Wuebbles, 2010) using PRISM (Parameter-elevation Rela-tionships on Independent Slopes Model; http://www.prism.oregon state.edu) 1961–1990 two km resolution climate normal (monthly temperature and precipitation) and CRU climate normal (monthly humidity) as the baseline climate (Daly et al., 2008). These coarse-resolution anomalies were then interpolated to the spatial resolution of the respective climate normal via a spline technique, and then added to (temperature) or multiplied by (precipitation and vapor pressure) the climate normals. The downscaled climate data were then interpolated to a 1 km resolution. The data and additional infor-mation on calculations are available from the Scenarios Network for Alaska and Arctic Planning (SNAP) data download website (https://www.snap.uaf.edu/tools/data-downloads). TSR was then used to model changes in annual and summer (i.e., June, July, and August) air temperature (T_{ANN}/year and T_{JJA}/year), precipitation (P_{ANN}/year and P_{JJA}/year), and vapor pressure deficit (VPD_{JJA}/year) from 1984 to 2015.

To account for potential topographic controls, we used elevation information from the National Elevation Dataset (NED; 60 m spatial resolution; http://ned.usgs.gov/) and computed a topographic ruggedness (TR) index (Riley, DeGloria, & Elliot, 1999). TR values clo-ser to one represent rugged landscapes, while smaller TR values rep-resent flatter landscapes. Information on the presence–absence of near-surface (within 1 m) permafrost (NSP_{EXT}; Pastick et al., 2015), excluding areas where permanent surface water has been observed, and soil texture (Jorgenson et al., 2008) were introduced because soil properties and conditions exert strong controls on vegetation and hydrology.

Overall, 16 environmental covariates were chosen based on our knowledge of factors likely to be associated with vegetation and sur-face-water dynamics, and data availability in Alaska (Table 1). Aver-age trend and covariate values were determined for each ecozone ($n = 29$), and nonparametric Locally Weighted Scatterplot Smoothers (LOWESS) were used to visually examine the nonlinear shape of response functions in a flexible manner. This information was then used to structure a variable and model selection procedure based on generalized additive modeling, using R (R Core Team, 2015). We focused our analysis on explanatory variables that had low correla-tion ($|r| \leq 0.5$) with each other and those significantly (p-value < 0.05) correlated with trends in vegetation productivity and surface-water dynamics.

2.5 | Predictive modeling and mapping of areas vulnerable to change

Classifier and map development consisted of data exploratory analy-ses, decision tree model calibration, and map assessments and strati-fied estimation of change extents. A boosted decision tree model (Quinlan, 1993) was used to estimate change/no-change occurrence using spectral change metrics (e.g., regression coefficients), a digital elevation model, and expert interpretations of land-surface change using time series of moderate and high-resolution imagery ($n = 430,000$). Decision tree classifiers are nonparametric classifiers that recursively partition a dataset into more homogenous subsets (i.e., nodes), while minimizing a cost function (e.g., Entropy), to pre-dict class membership (e.g., change, no change). For the change and no-change product, a boosted decision tree methodology was employed using a commercial version (See5) of the C4.5 algorithm

TABLE 1 List of the 16 environmental covariates originally considered for inclusion in the models of regional controls on vegetation productivity and surface-water dynamics

Variable	Unit	Description
Elev.	m	Elevation
TR	m	Topographic ruggedness
NSP_{EXT}	%	Near-surface (within 1 m) permafrost extent
Silty	%	Silty soil extent
Sandy	%	Sandy soil extent
Rocky	%	Rocky soil extent
P_{ANN}	mm	Total annual precipitation
P_{ANN}/year	mm/year	Change in total annual precipitation
P_{JJA}	mm	Total summer precipitation
P_{JJA}/year	mm/year	Change in total summer precipitation
T_{ANN}	°C	Mean annual temperature
T_{ANN}/year	°C/year	Change in mean annual temperature
T_{JJA}	°C	Mean summer temperature
T_{JJA}/year	°C/year	Change in mean summer temperature
VPD_{JJA}	kPa	Mean summer vapor pressure deficit
VPD_{JJA}/year	kPa/year	Change in summer vapor pressure deficit

(Quinlan, 1993). Ensemble learning methods are robust to the presence of noise (e.g., incorrect class labels, feature [attribute] noise), especially when methods for avoiding overfitting are employed. Thus, pre- and postpruning techniques (i.e., case constraints and statistical confidence pruning) were used to prevent model overfitting tendencies (Quinlan, 1986), and overfitting avoidance was assumed to be sufficient to deal with potential label and feature noise.

Feature attribute selection was done using domain knowledge, impurity measures, and interpretations of change type. Model accuracies were assessed using f-fold cross validation. Decision tree models were applied to useful predictor variables to produce maps of change occurrence throughout Alaska. A two-stage sampling design was used to independently assess map accuracies, improve precision of change extent estimates, and provide associated confidence intervals. In the first stage of our two-stage sampling design, 50 primary sampling units were selected randomly from grids (5 × 5 km) covered with aerial photographs and high-resolution imagery (Figure 1). In the second stage, sample pixels were selected within each grid and distributed between mapped change ($n = 2452$) and no change ($n = 635$) strata to interpret change type and meet our specified margin of overall error ($SE = 0.01$). Validation samples are independent of model training samples described above. The map and reference data were used in conjunction to generate error matrices for accuracy assessment as well as for estimating area of change and confidence intervals using estimators described in Olofsson et al. (2014) and Gallaun et al. (2015).

3 | RESULTS

3.1 | Attribution of spectral index changes

To assign change causation at the local scale, we compared trends in late-season multispectral indices (Figure 2) to interpretations of ecological and geomorphological change (or no change) mapped with high-resolution imagery. Here, we highlight a portion of the major change processes that occur across a diverse suite of ecosystems in Alaska. Detected changes include, but are not limited to, shrub and tree expansion, fluvial, coastal, and lacustrine dynamics (i.e., flooding/expansion, drying/drainage), thermokarst, glacial retreat and expansion, vegetation and geomorphic succession, wildfires, insect damage, and anthropogenic disturbances.

3.2 | Shrub and tree expansion

Shrub expansion on tundra and wetland communities was observed at 15 sites (145 interpretations) within the Arctic Network of Parks (ARCN) and resulted in an average increase in vegetation productivity index (0.002 ± 0.0002 Standard Error (SE) NDVI/year), which was significantly ($p < 0.0001$) higher than the average change in vegetation productivity (0.0001 ± 0.0 NDVI/year) for the other 447 interpretations of no change at the same sites (Supporting Information Figure S2a). Reduction in shrub extent due to floodplain erosion was only observed at one site (21 interpretations) within the ARCN

and resulted in an average decrease in vegetation productivity (-0.0043 ± 0.0007 NDVI/year), which was not significantly different than the average value (-0.0046 ± 0.0012 NDVI/year) at 16 locations of no change at the same site.

Shrub expansion was also observed at two sites (23 interpretations) within the boreal zone of the Arctic National Wildlife Refuge (ANWR) and resulted in an average increase in vegetation productivity index (0.002 ± 0.0002 NDVI/year), which was not significantly ($p = 0.13$) different than the average trend (0.001 ± 0.0002 NDVI/year) for the other 147 interpretations of no change at the same sites. Likewise, tree expansion was observed at one site (22 interpretations) within the boreal region of ANWR and resulted in an average greening trend (0.002 ± 0.0002 NDVI/year) that was not significantly different than the average trend (0.002 ± 0.0001 NDVI/year) for the other 70 interpretations of no change at the same site. Identifying shrub and tree expansion at the Landsat pixel scale can be challenging, because expansion can result in sparsely distributed patches of vegetation with low stand densities, and greening trends may be associated with enhanced tree growth in forested stands that would be difficult to manually detect from two dates of high-resolution imagery.

3.3 | Fluvial, coastal, and lacustrine dynamics

Erosion and depositional processes resulted in distinct wetting and drying trends within riverine, lacustrine, and coastal areas of Alaska. For example, coastal erosion and deposition along the Alaskan Arctic coastline of the Northern Teshekpuk Lake Special Area (Jones et al., 2009) resulted (on average) in a large decrease (-0.007 ± 0.0 NDWI/year) and increase (0.014 ± 0.0 NDWI/year) in NDWI values, respectively. Furthermore, river erosion was observed at two sites (10 interpretations) within the Tanana-Kuskokwim Lowlands (Jorgenson, Shur, & Pullman, 2006) and resulted in an average wetting trend (0.01 ± 0.002 NDWI/year), which was significantly different than slope values (-0.0004 ± 0.0 NDWI/year) observed at 153 locations with no change at the same sites (Supporting Information Figure S2b). Likewise, thermokarst lake expansion and drainage events that have been observed on the Bering Land Bridge National Preserve (Jones et al., 2011) resulted (on average) in wetting (0.007 ± 0.0002 NDWI/year) and drying (-0.03 ± 0.0002 NDWI/year) trends, respectively.

3.4 | Thermokarst

Thermokarst associated with the collapse of permafrost plateaus was observed at three sites (10 interpretations) within the Tanana Flats and resulted in an average wetting trend (0.0014 ± 0.001 NDWI/year), which was significantly different ($p < 0.005$) than the average slope values (-0.0009 ± 0.0 NDWI/year) for the other 178 interpretations of no change at the same sites (Supporting Information Figure S2c). Thermokarst occurrence due to ice-wedge degradation was observed at 12 sites (122 interpretations) within the Arctic National Wildlife Refuge (ANWR) (primarily occurring in coastal and lowland areas) and resulted in an average increase
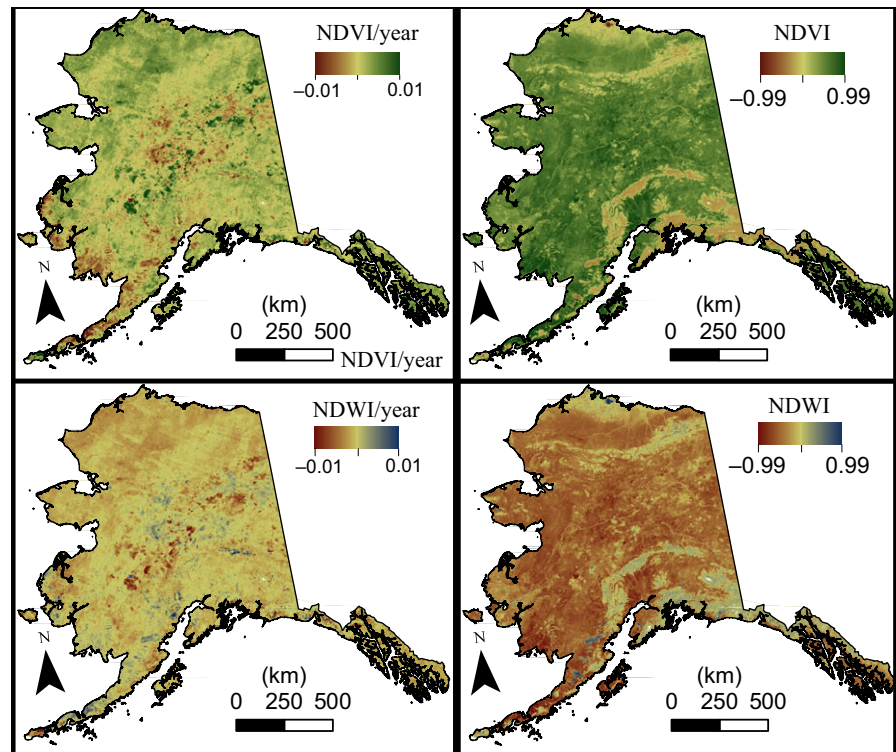
FIGURE 2 Trend slope (left) and offset (right) maps (30 m spatial resolution) produced from peak-growing season (July and August) Landsat-based multispectral indices (i.e., Normalized Difference Vegetation Index [NDVI], Normalized Difference Wetness Index [NDWI]). Offset represents model estimates of spectral indices in 1984

(0.003 ± 0.0001 NDVI/year) in vegetation productivity, which was significantly ($p < 0.005$) different than the average change in vegetation productivity (0.002 ± 0.0 NDVI/year) for the other 978 interpretations of no change at the same sites (Supporting Information Figure S2d). Note that while trends can be statistically different, there can be a substantial amount of overlap between class values and the chance of finding significant differences increases as the number of observations increase.

Larger thermokarst features and ecological responses are well depicted within the Landsat-based trend and change products. Retrogressive thaw slumps (RTS) and active-layer detachments slides (ALDs) having occurred in the ARCN ($n = 2,970$), as mapped by Swanson (2014), resulted (on average) in significantly ($p < 0.0001$) different browning (−0.001 ± 0.0 NDVI/year) and greening trends (0.001 ± 0.0 NDVI/year), respectively (Supporting Information Figure S2e). Divergent trends likely reflect differences in the time of initiation, duration, and associated ecological response. That is, both RTS and ALDs exposed bare soil, but ALDs are rapid, narrow, one-time events allowing recovery to be initiated quickly, whereas, RTS tend to broader and remain active over many years.

3.5 | Glacier retreat and expansion

Glacial cover has diminished on approximately 3,725 km² of Alaskan national parks over the last-half century (Loso et al., 2014) and the spectral signatures associated with these changes are evident within our trend analysis. Accumulation of vegetation on glacial till, typically occurring near the terminus after glacial retreat in Alaska, results (on average) in distinct greening trends (0.0025 ± 0.0 NDVI/year).

Proglacial lake formation (as identified using data from Pekel et al., 2016 and Loso et al., 2014) results (on average) in clear wetting trends (0.008 ± 0.0009 NDWI/year). Recent transitions from perennial ice to debris cover appears to result in both decreasing and increasing trends (Supporting Information Figure S3), but detailed land-cover conversion and timing information is not available so we cannot provide a quantitative summary. While glacial expansion may have occurred over a smaller area of Alaska, we do not summarize trend values here because these changes are mostly artifacts of unmapped glaciers due to inadequate historical imagery. However, glacial expansion would result in trends inverse of those discussed above, the magnitudes of which would depend on the type of land-cover conversion (e.g., debris cover to perennial ice, water to perennial ice). Lastly, stable glaciers had (on average) no trend.

3.6 | Wildfires, insects, and timber harvesting

Fire is the dominant landscape-scale disturbance operating on annual timescales in Alaska, having occurred on approximately 240,000 km² of the landscape from 1950 to 2015 according to the Bureau of Land Management (BLM) Large Fire Database. The impacts of fire on vegetation productivity are clearly demonstrated within our trend analyses at the regional scale (Supporting Information Figure S4). Postfire recovery patterns, as depicted by our successional chronosequence (Adjusted $R^2 = 0.79$; $p < 0.0001$; Figure 3a), are nonlinear and suggest a rapid increase in vegetation productivity until 20 years after fire occurrence (a period associated with establishment of productive deciduous vegetation), a slight decrease in
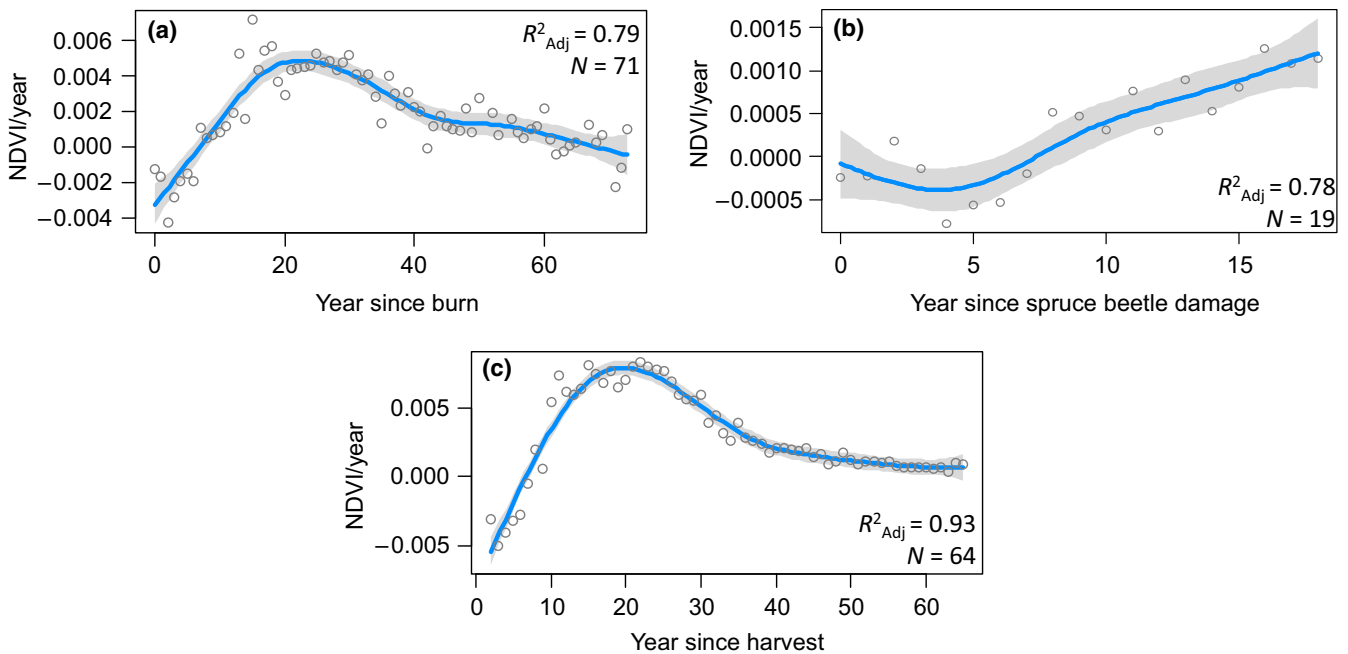
FIGURE 3 Mean change in vegetation productivity (NDVI/year) as a response of year since (a) fire (b) spruce beetle damage, and (c) harvest. Data were fit with a generalized additive model (GAM) using cubic regression splines through the mean value of each year. Data points at "Year since disturbance" 0 represent stands where disturbance occurred at year 2015, according to the Bureau of Land Management (BLM) Large Fire Database, United States Department of Agriculture's National Insect and Disease Survey data, and United States Forest Service timber harvest dataset. Shaded areas represents confidence interval ($\alpha = 0.05$) of the GAM

increasing productivity levels after 30 years (a period associated with deciduous/coniferous mixing), and another decrease around 60 years after fire (a period associated with increased dominance of mature spruce forest). Fires (on average) resulted in an overall increase in photosynthetic activity (0.13 NDVI) over 75 years, as determined by calculating the integral of the response function in Figure 3a. The response of vegetation productivity after fire may also be associated with soil conditions, where large greening trends appear to be most prevalent within nutrient-loess soils, in addition to time of burning, fire severity, and prefire vegetation composition.

Insect-induced mortality has been observed on approximately 14,000 km^2 of Alaska since 1997, according to the United States Department of Agriculture's National Insect and Disease Survey Database, occurring in both the interior boreal forests as well as the Alaska Range taiga regions and transition forests near the southern Alaska coast. Spruce beetle infestation generally reduces canopy densities and vegetation productivity shortly after occurrence, as is reflected in our chronosequence model (Adjusted $R^2 = 0.78$; $p < 0.001$), but increases in vegetation productivity are also associated with forests recovering from insect damage (Figure 3b). In some cases, productivity levels after insect outbreaks can exceed preoutbreak levels. For example, recovery from insect damage (primarily caused by spruce bark beetles) observed within the wilderness area of the Kenai National Wildlife Refuge during the late 1980s and 1990s resulted in an average increase in vegetation productivity (0.001 ± 0.0 NDVI/year), which was significantly higher ($p < 0.0001$) than the average rates (−0.0004 ± 0.0 NDVI/year) at locations with no change (Supporting Information Figure S2f).

Forest harvesting impacts in Alaska resulted in substantial changes to vegetation productivity, and are estimated to have occurred on approximately 2,200 km^2 of the Tongass and Chugach National Forests from 1950 to 2015 according to the United States Forest Service timber harvest database. Browning trends are largely associated with areas that have been recently (<7 years) harvested and greening trends correspond to stands that are regenerating (>7 years) (Figure 3c). In this chronosequence model (Adjusted $R^2 = 0.93$; $p < 0.0001$), vegetation productivity rapidly increased until 15–20 years after harvest and then increased at a decreasing rate and leveled off thereafter. Forest harvesting (on average) results in an overall increase in vegetation productivity (0.19 NDVI) over the observed period. Compared to fires and insects, at time zero there is typically no residual biomass to confound the time series, and the time series (age of the stand) is more easily established. In all cases the chronosequences clearly demonstrate the effect of disturbances on changes in vegetation productivity levels, despite confounding issues associated with site-specific factors (e.g., soil properties) and shifts in the climate which were not included in the experimental design.

3.7 | Regional patterns and drivers of change

3.7.1 | Terrestrial surface dynamics

The Arctic Tundra ecoregion has seen the largest increases in T_{ANN} during the 32 year period (0.06 °C/year), followed by the Bering Tundra (0.05 °C/year), Intermontane Boreal (0.04 °C/year), Bering Taiga and Alaska Range Transition (0.03 °C/year), Coastal

Rainforests, and the Pacific and Coast Mountain Transition ecoregion (<0.025 °C/year). Trends in late-season vegetation productivity (NDVI$_{JA}$/year), however, best correlate with changes in mean summer air temperatures and change in vapor pressure deficit (Supporting Information Figure S5). That is, T$_{JJA}$/year and VPD$_{JJA}$/year contribute to changes in vegetation productivity, where increases in summer temperature and vapor pressure deficit correspond well to linear and nonlinear increases and decreases in vegetation productivity, respectively (Figure 4). These variables explain 75% of the variation in changing vegetation productivity levels, suggesting that regional, late-season vegetation productivity trends are largely driven by climatic change throughout Alaska.

3.7.2 | Surface-water dynamics

The total area of permanent surface water has generally increased throughout Alaska, with a significant amount of interannual and spatial variability reflecting complex interplays among topography, geomorphology, and hydro-climatic factors (Figure 5 and Supporting Information Figure S5). Of the 47,258 summary grids, approximately 15,000 and 4,000 have significant ($p < 0.05$) increasing and decreasing trends with time, respectively. Distinct clusters of increasing

trends correspond to surface-water gains that have generally occurred in lowlands and areas underlain by permafrost that have experienced the largest increases in T$_{ANN}$ (Figure 6). Conversely, areas with surface-water loss are generally isolated, although there is notable clustering in rocky uplands in southern Alaska, the western tip of the Seward Peninsula, the southeastern portion of the Yukon-Kuskokwim Delta, and along sand sheets of the Yukon-Old Crow Basin.

3.8 | Change type classification and validation

A total of 29 environmental covariates were used during change detection model development (Supporting Information Table S1). Overall training and cross-validation accuracies for the calibrated change model were 99% and 98%, respectively. The decision tree model was applied to useful environmental predictor variables to construct a map of the probability of change occurrence (Figure 7; Pastick et al., 2018) based on decision tree ensemble estimates of change occurrence and posterior confidence estimates. Independent interpretations and the change map were used to construct a confusion matrix and calculate area class estimates and associated confidence intervals. In addition to overall accuracy (95.8%), the
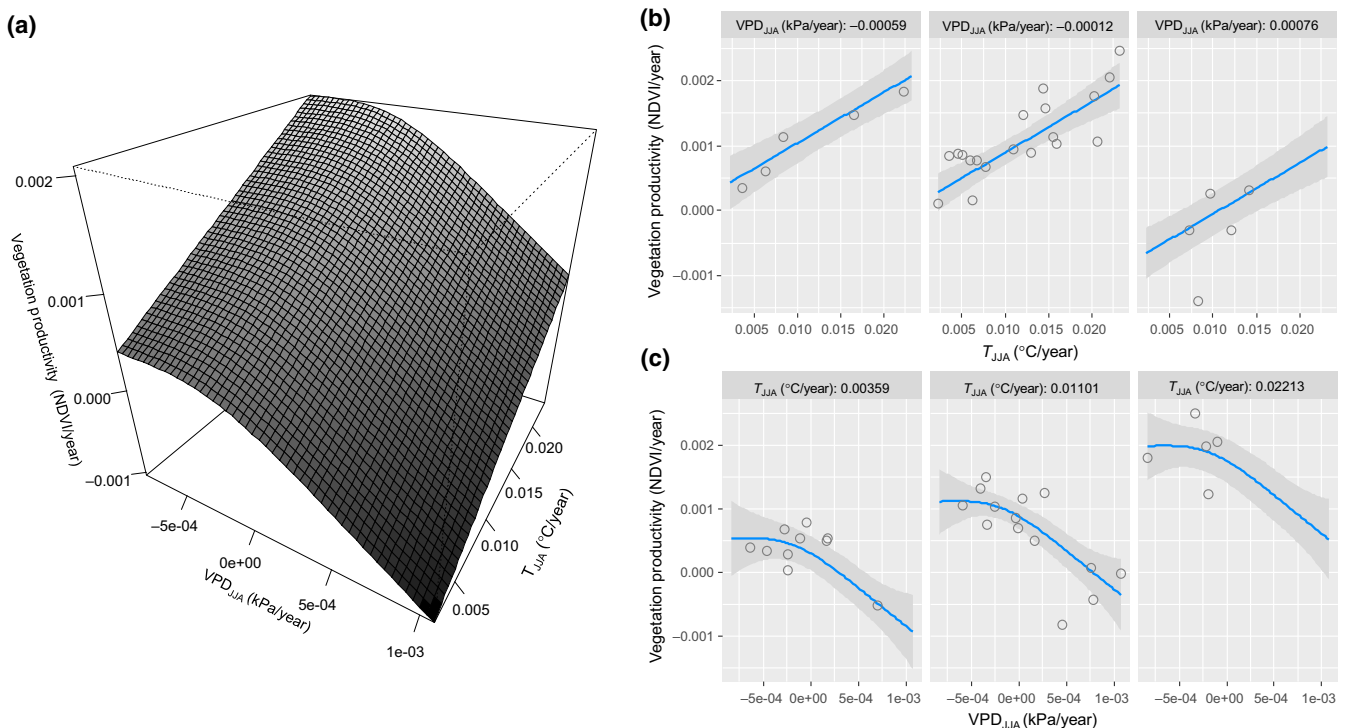

FIGURE 4 Surface (a) and cross-sectional plots (b, c) showing the relationships between mean changes in late-season vegetation productivity (NDVI$_{JA}$/year), mean summer temperature (T$_{JJA}$; °C/year), and vapor pressure deficit (VPD$_{JJA}$; kPa/year) for ecozones of Alaska (Nowacki et al., 2003; $n = 29$), as described by a generalized additive model (GAM) using cubic regression splines (Adjusted $R^2 = 0.72$). Cross-sectional plots depict the relationship between changes in vegetation productivity and T$_{JJA}$ (b) or VPD$_{JJA}$ (c) for a subset of values within the other grouping climate variable. Cross sections are defined by values of the grouping variable such that partial residuals appear only once in the grouping panel they are closest to. Shaded areas represents confidence interval ($\alpha = 0.05$) of the GAM. The black to white color gradient of the response surface (a) reflect lower and higher trend values (NDVI$_{JA}$/year), respectively

Stable surface water

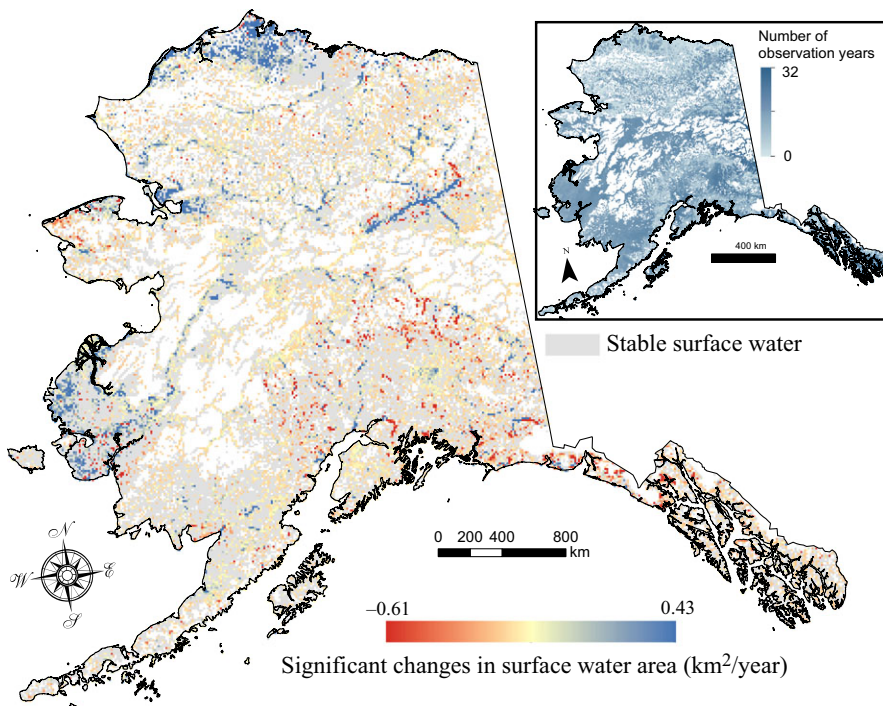Significant changes in surface water area (km²/year)

FIGURE 5 Direction and magnitude of significant (p-value < 0.05) changes in annual permanent surface water area as derived from linear regression analysis. Trends are derived from years (inset) where the unobserved component of the maximum permanent water extent is less than 5%. Areas in white and gray represent areas where permanent surface water has never been observed and stable water surfaces, respectively, over the study period (1984–2015)
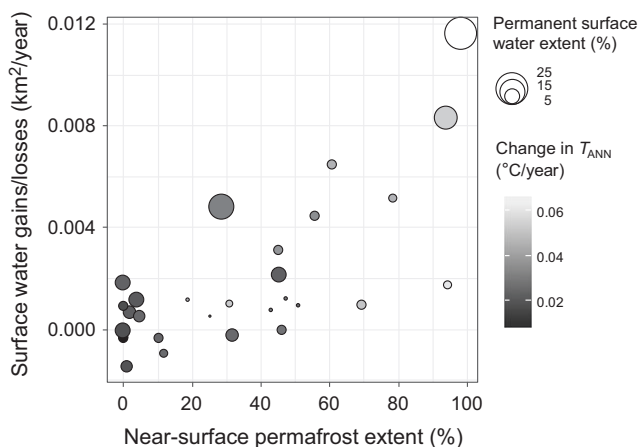

FIGURE 6 Average permanent surface water area loss and gains (km²/year) as a function of near-surface (within 1 m) permafrost extent (Pastick et al., 2015) in ecozones (Nowacki et al., 2003; $n = 29$) of Alaska. Bubble sizes and colors correspond to maximum permanent surface water extent (%) and average changes in T_{ANN} (°C/year) within each ecozone, where larger and whiter circles represent bigger water extents with more historic (1984–2015) warming

estimated confusion matrix (Table 2) depicts distinct errors or accuracies as they relate to each class prediction. Map estimates of the no change class (probability <50%) had much higher user accuracies than those of the change class (97.6% vs. 83.5%), and lower producer's accuracies for areas having undergone some change (97.6% vs. 83.7%). According to our best estimate, approximately 13% (~174,000 km²; 95% CI = 165,000 km², 182,000 km²) of Alaska has undergone some change during 1984–2015. The majority of change processes occurred in lowlands and coastal, riverine, and boreal

ecosystems. The ecoregion with the highest vulnerability to change is the Intermontane Boreal (29%), followed by the Pacific Mountain Transition (9.9%), Bering Taiga (8.6%), Alaska Range Transition (5.9%), Coastal Rainforest (5.9%), Bering Tundra (2.5%), Coast Mountains Transition (2.5%), Arctic Tundra (2.2%) (Table 3).

4 | DISCUSSION

4.1 | Vegetation expansion and growth

Our observations of vegetation growth are in agreement with historical increases in vegetation productivity and expansion inferred from field and remote sensing studies (Loranty et al., 2016; Myers-Smith et al., 2011; Beck & Goetz, 2011; Walker et al., 2009; Figure 4a). Tundra shrubification can lower surface reflectance, increase evapotranspiration, and affect snow redistribution and aboveground carbon stocks (Loranty & Goetz, 2012; Sturm, Douglas, Racine, & Liston, 2005), which may result in regional air/ground temperature increases and active layer thickening associated with permafrost degradation (Bonfils et al., 2012; Euskirchen et al., 2016; Lawrence & Swenson, 2011). Expansion of boreal forest into Arctic and alpine ecosystems has also been attributed to high-latitude warming and can increase the amount of atmospheric heating that occurs (Chapin, Eugster, McFadden, Lynch, & Walker, 2000), which may provide feedbacks to regional and global climates depending on the rate and extent of treeline advance (Euskirchen et al., 2016; Pearson et al., 2013; Zhang et al., 2013).

Warming has also indirectly promoted vegetation growth through the formation of terrestrial land surfaces for example, as the result of glacier retreat (Supporting Information Figure S3) where
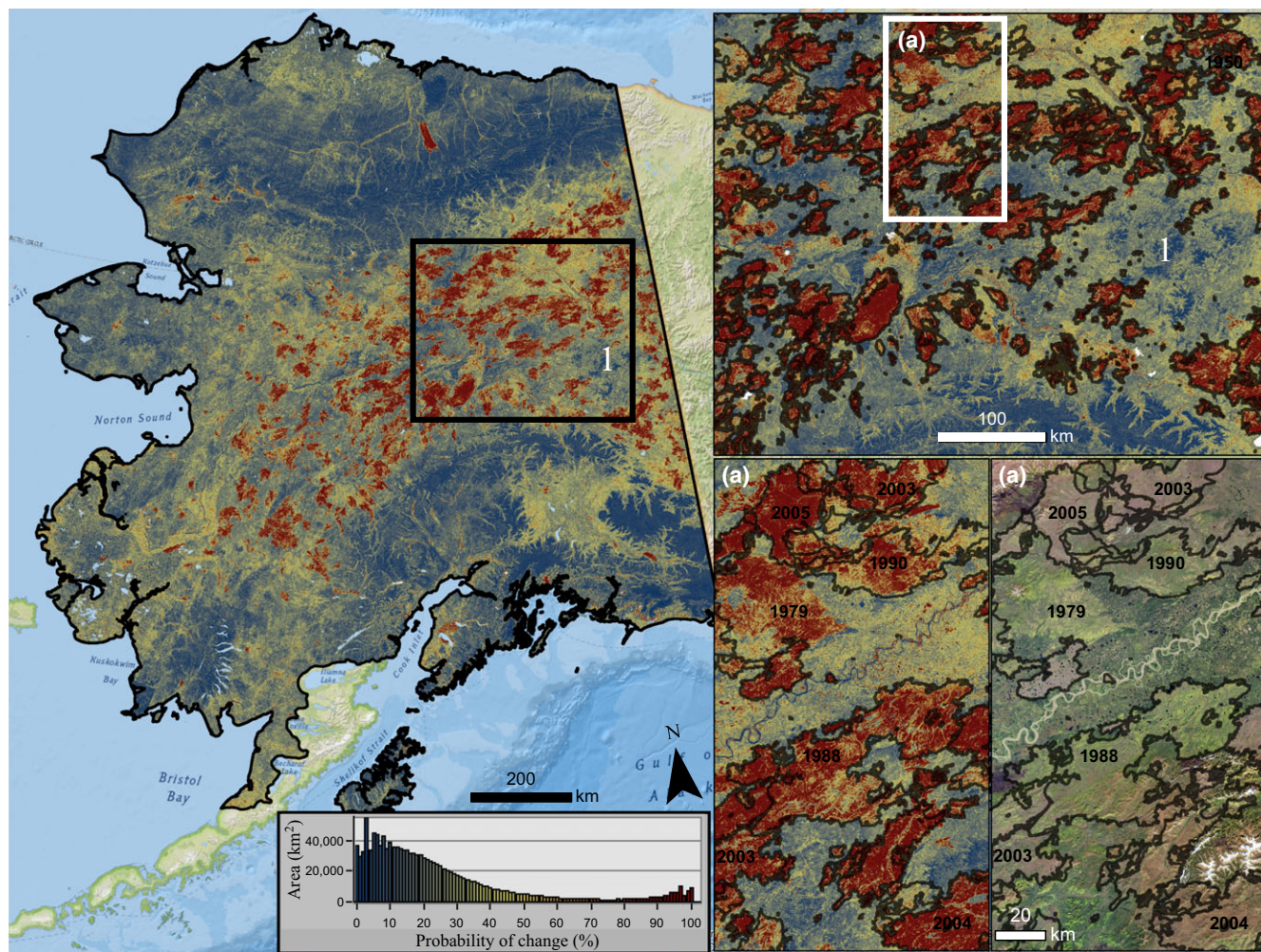
FIGURE 7 Predictions of the probability (%) of change occurrence (30 m spatial resolution), derived from a boosted decision tree model using spectral change metrics, a digital elevation model, and manual-image interpretations (Figure 1) of change type. Insets show fire boundaries from the Bureau of Land Management (BLM) Large Fire Database and Landsat 8 imagery (bottom right; 2016) north of Fairbanks, Alaska

TABLE 2 Estimated error matrix (percent of area) and associated accuracy statistics and standard errors (*p*-value < 0.5). Column totals correspond to estimated area proportions calculated using reference and mapped data

	Reference		Row total	User's accuracy
	No change	Some change		
Map				
No change	85	2.1	87.1	97.6 ± 0.6
Some change	2.1	10.8	12.9	83.5 ± 2.8
Column total	87.1	12.9	–	–
Producer's accuracy	97.6 ± 3	83.7 ± 1	–	–
Overall accuracy	–	–	–	95.8 ± 2

vegetation succession influences sediment availability, ground water runoff, and soil properties (Klaar et al., 2015). If Alaska continues to warm as expected, wildfire and thermokarst may also increase in frequency and extent, which can create mineral-rich seedbeds that are conducive for shrub colonization (Lantz, Kokelj, Gergel, & Henry,

2009). Our results (Figure 4a) confirm the idea that continued warming will increase aboveground biomass throughout portions of Alaska (Ackerman, Griffin, Hobbie, & Finlay, 2017), which may partly help curb carbon emissions from thawing permafrost (Abbott et al., 2016). In contrast, our results (Figure 4c) also suggest that plant productivity may decline in warming regions due to drought stress which would predispose woody vegetation to the risk of disease, fire, and mortality (Rogers et al., 2018; Trugman, Medvigy, Anderegg, & Pacala, 2018). Further research is needed to better understand climates impact on short and long term shifts in vegetation phenology, as well as to identify and quantify higher order interactions among environmental factors (e.g., climate, soil moisture) that influence vegetation productivity at a multitude of scales.

4.2 | Fluvial, coastal, lacustrine, and surface-water dynamics

This study also provides evidence for substantial changes in ecosystem structure as the result of erosion and deposition processes that

TABLE 3 Change statistics within major ecoregions (Nowacki et al., 2003) of Alaska

Ecoregion	Land area (km^2)	Mapped change area (km^2)	L_c (%)
Intermontane Boreal	469,206	135,040	28.8
Bering Taiga	201,985	17,425	8.6
Coastal Rainforests	179,673	10,546	5.9
Alaska Range Transition	159,905	9,405	5.9
Arctic Tundra	300,850	6,698	2.2
Pacific Mountains Transition	18,829	1,880	9.9
Bering Tundra	60,481	1,526	2.5
Coast Mountains Transition	19,315	481	2.5

L_c = change area fraction = (total change area/total land area) × 100.

have occurred throughout coastal and riverine ecosystems in Alaska. In our analysis, approximately 700 km^2 of the study area within 200 m of the coastline (modified from Nowacki et al., 2003), and where permanent surface water has ever been observed, experienced change (mainly coastal erosion and accretion), with the majority of change occurring along permafrost-dominated coastlines of the Beaufort Coastal Plains and Yukon-Kuskokwim Delta. Increasing coastline erosion rates (Jones et al., 2011) have been attributed to a number of factors, such as shifts in storm winds, record declines in Arctic sea ice (Stroeve et al., 2008), sea-level rise (Steele, Ermold, & Zhang, 2008), and terrestrial permafrost degradation (Jorgenson et al., 2006). Coastal transgression can result in increased sediment and carbon flux to oceans (Hayes, Guo, & McGuire, 2007; Jorgenson & Brown, 2005), changes to wildlife habitat (Flint et al., 2008; Tape, Flint, Meixell, & Gaglioti, 2013), loss of historical and cultural sites (Jones, Hinkel, Arp, & Eisner, 2008), and damage to infrastructure (Houseknecht & Bird, 2006).

Surface-water gains can occur through erosion of lake shorelines, thermokarst, and flooding events. Our finding of significant surface-water gains in warming tundra ecozones (Figure 6) is consistent with reports of increasing rates of thermokarst and lake expansion in these areas (Jorgenson et al., 2001), where thaw is dominated by lateral heat fluxes at the margins of water bodies, which have not seen significant increases in precipitation over the last three decades (Supporting Information Figure S5). Conversely, surface-water losses can be caused by degrading permafrost leading to gradual or catastrophic drainage of lakes and other fluvial geomorphological processes as observed in our analyses (Figure 5). Surface-water declines in Arctic lowlands have been attributed to lateral surface drainage events (Hinkel et al., 2007; Jones et al., 2011), which results in water being redistributed to surrounding low points on the landscape, subsurface drainage (Yoshikawa & Hinzman, 2003), and terrestrialization of lake surfaces that have likely been enhanced by a warming climate (Figure 4a).

Surface-water gains in boreal regions of Alaska are largely driven by ice-jam flooding events, as is captured in our trend analysis (Figure 5), which have recharged lake basins within riverine and lowland

flood plains along the Yukon River (Duguay, Bernier, Gauthier, & Kouraev, 2015; Jepsen, Walvoord, Voss, & Rover, 2016). Increases in groundwater discharge, as a result of enhanced permafrost thaw, are likely a contributing factor to surface-water gains in riverine corridors (Walvoord, Voss, & Wellman, 2012). Surface-water loss has also occurred in isolated patches throughout boreal landscapes and is indicative of exogenetic processes, such as subterraneous drainage, paludification (Jorgenson & Osterkamp, 2005), and lake infilling and tapping. Surface-water loss leading to (or promoted by) terrestrial (aquatic) vegetation colonization and increasing rates of lake surface loss may be due to recent warming trends and evaporative loss (Roach, Griffith, & Verbyla, 2013; Roach, Griffith, Verbyla, & Jones, 2011), which can impact the local climate, wildlife habitat, and socio-economics (Hinzman et al., 2005).

The decline in surface water areas in south-central Alaska co-occurs with long-term declines in annual precipitation (Supporting Information Figure S5) that can substantially reduce precipitation runoff and mean annual water balances. Spatially homogenous surface-water trends are typically the result of temporal trends in hydro-climatic factors (Karlsson, Lyon, & Destouni, 2012), consistent with observations made in the Kenai Peninsula over the last half century (Klein, Berg, & Dial, 2005), but also likely reflect the influence of glaciers in southern Alaska. Observed surface water trends do not support the generalization of surface water extents increasing and decreasing in continuous and discontinuous permafrost regions (Smith, Sheng, & MacDonald, 2007), respectively, and suggest that trends are substantially moderated by local conditions and processes. This finding is consistent with previous research (Karlsson, Jaramillo, & Destouni, 2015) and highlights complexities associated with better understanding mechanisms that influence surface-water dynamics across heterogeneous permafrost landscapes.

4.3 | Thermokarst

Recent increases in the rate of thermokarst occurrence in tundra and boreal ecozones of Alaska have been linked to unusually warm summer weather and heavy rainfall (Balser, Jones, & Gens, 2014; Jorgenson et al., 2015; Lara et al., 2016). Our finding of increased rates of vegetation productivity after ice-wedge degradation may reflect colonization of thermokarst troughs by highly productive sedges (Supporting Information Figure S2c), whereas browning trends associated with thermokarst (e.g., permafrost plateau collapse) are likely caused by increasing wetness due to water pooling (Reynolds & Walker, 2016). Identification and attribution of mechanisms responsible for thermokarst disturbance is nevertheless difficult because of the fine-spatial scale at which this phenomenon occurs (generally smaller than a Landsat pixel), co-occurrence with other disturbances, poor understanding of geology (e.g., ice content), and modest changes in reflectance values associated with thermokarst and water impoundment that can be obscured by vegetation. Thus, identification of certain thermokarst features typically requires high-resolution spectral or topographic (e.g., LiDAR) data that can be used

to directly or indirectly resolve changes in land-surface features (Jones et al., 2015, 2016). It is important to point out that shifts in subsurface hydrology due to permafrost thaw could also result in browning trends, where soil moisture declines can result in the drying of plants; however, we are not aware of any widespread reports of such changes and attribution would require field data.

4.4 | Glacial retreat and expansion

Rising temperatures, declining snowfall, and mechanical processes (e.g., calving glacier dynamics) have driven a reduction in the area and volume of the majority of glaciers in Alaska (Berthier, Schiefer, Clarke, Menounos, & Rémy, 2010; Larsen, Motyka, Arendt, Echelmeyer, & Geissler, 2007; Larsen et al., 2015), which has led to the formation of proglacial lakes, ruby moraines, and outwash floodplains that are colonized by pioneer species (Chapin, Walker, Fastie, & Sharman, 1994; Sommaruga, 2015; Supporting Information Figure S2), a trend that is expected to continue over the 21st century (McGrath, Sass, O'Neel, Arendt, & Kienholz, 2017). Our areal estimates of change in historically glaciated regions of Alaska are in global concordance with previous estimates made by Loso et al. (2014) ($R^2 = 0.90$; $p < 0.005$; Supporting Information Figure S6), although differences in study periods result in substantially lower estimates within our analysis. Receding glaciers and declining snow cover promote upward migration of species and communities in mountains (Gottfried et al., 2012), as is observed in our analysis, as well as influence downstream aquatic ecosystems by governing flow regimes (Brown & Mote, 2009), erosion rates, sediment and nutrient flux (Hallet, Hunter, & Bogen, 1996), and water quality and temperature (Brown & Milner, 2012; Fellman et al., 2015). Seasonal water releases from alpine glaciers provide vital ecosystem services and resources that are essential for human welfare, and are expected to increase (decrease) in the short term (medium to long term) with rising air temperatures, lengthening of the snow-free season, decreasing snow-to-rain ratios, and increased radiative forcing (Huss et al., 2017).

Glacier changes documented in Alaska serve as an indicator of climatic change and reemphasize the need to develop automated approaches for characterizing glacial advance/retreat and associated areal coverage. While manual interpretation of aerial and satellite imagery has frequently been used for glacier change analysis, the use of large, multitemporal stacks of optical satellite data has only recently been explored (Winsvold, Kaab, & Nuth, 2016). Given the distinct spectral response of stable perennial ice, glacier retreat, and associated ecological processes (e.g., succession), our results further demonstrate that Landsat-based trend maps are a useful tool for mapping glacial change and ecosystem response, although we recognize the problem of debris accumulation over glacial ice remains a persistent problem in defining the lower boundaries of glaciers. Holistic data fusion approaches that effectively leverage information obtained from passive, active, and geophysical sensors (e.g., Landsat, Sentinel, ICESat-2) will improve our ability to fingerprint glacial change, and image-segmentation techniques could be applied to multitemporal products to explicitly incorporate contextual information

that pixel-based classifiers typically neglect or implicitly account for (Robson et al., 2015).

4.5 | Wildfires, insects, and timber harvesting

Recent climate warming has been linked to changes in the fire regime in Alaska (Calef, Varvak, McGuire, Chapin, & Reinhold, 2015; Duffy, Walsh, Graham, Mann, & Rupp, 2005; Rocha et al., 2012), and wildfires play a major role in determining the rates, trajectories, and duration of successional development in Arctic tundra and boreal forests (Figure 3a). Results of our chronosequence model aligns with the findings of others (e.g., Bond-Lamberty, Wang, & Gower, 2004; Kasischke & French, 1997), where establishment of woody vegetation and peak productivity rates occurred approximately 20 years after a fire in black spruce stands, the prevailing fuel load in boreal regions of Alaska, and spruce trees were expected to dominate the forest canopy approximately 30–40 years after fire. Whether this mean rate of postfire succession, or changes to alternative trajectories with more deciduous trees, will continue in a warming environment is largely contingent on future fire severity (e.g., amount of residual organic soil layer remaining after fire), fire return intervals, permafrost, and site moisture (Alexander, Mack, Goetz, Beck, & Belshe, 2012; Beck et al., 2011; Johnstone, Hollingsworth, Chapin, & Mack, 2010).

Wildfires also play an important role in the rate and extent of vegetation growth and productivity of a site. Analysis of vegetation productivity trends and estimates of aboveground biomass postfire, as derived from remote sensing (Margolis et al., 2015), indicate a potential relation between postfire productivity and biomass that warrants further investigation (Supporting Information Figure S7). Fire-induced changes have substantial implications for feedbacks to climate, in addition to physical structure where thinning may create more shadows and browning trends, and biophysical processes. For example, wildland fires often reduce albedo shortly after occurrence, result in a pulse of nutrients (e.g., nitrogen) that become available for uptake by plants, and provide the opportunity for deciduous forests to develop (as is reflected in our successional chronosequence), which generally raises surface albedo and increases the proportion of energy released to the atmosphere as latent heat (Chapin et al., 2010; Johnstone, Rupp, Olson, & Verbyla, 2011). A shift from a spruce to deciduous dominated landscape could act as a negative feedback to climate warming and increasing fire activity in boreal forests (Pastick et al., 2017; Rogers, Randerson, & Bonan, 2013).

Climate warming in boreal Alaska has also resulted in increased woody vegetation mortality from insects over recent decades (Berg et al., 2006; Soja et al., 2007), and projected warming is expected to increase outbreaks in western North America (Bentz et al., 2010). Biotic disturbance agents, such as bark beetle species (e.g., *Dendroctonus rufipennis*) and defoliators, can cause tree mortality or injure trees and predispose them to mortality from other stresses (Malmström & Raffa, 2000). While insect damage generally reduces vegetation productivity shortly after occurrence, by causing mortality or reducing canopy density, our findings suggest that areas

recovering from insect-induced mortality generally have higher productivity levels than preoutbreak conditions (Figure 3b). This could partly be in response to timber salvage postinfestation (Jones, 2008), but our results are corroborated by previous studies where vegetation productivity in beetle-affected stands either returned to preoutbreak levels following a brief recovery period (10–15 years), or exceeded preoutbreak conditions (Hicke, Johnson, Hayes, & Preisler, 2012; Romme, Knight, & Yavitt, 1986), which could reflect a shift in forest age class. However, additional work is needed to characterize the magnitude and extent of insect damage because of difficulties related to establishing time of occurrence and co-occurrence with other stresses (e.g., drought stress).

Logging in southern coastal Alaska has led to extensive changes to land-surface properties and biological processes (Zhou, Schroder, McGuire, & Zhu, 2016). Rapid tree regeneration is thought to result in canopy closure 15–25 years after clearcutting on productive forest soils (Sigman, 1985), corresponding to peak rates of vegetation productivity in our chronosequence model (Figure 3c), followed by a long-lasting stage of stem exclusion (Alaback, 1982; Deal & Farr, 1994) that generally has negative consequences for biodiversity and wildlife habitat (Dellasala et al., 1996). While harvesting reduces aboveground carbon stocks by removing wood from the ecosystem, it can increase photosynthetic activity, the amount of solar radiation that reaches the forest floor, soil temperatures, and rates of decomposition of soil organic matter (Sigman, 1985).

4.6 | Future directions and current limitations

Our approach to quantify change processes has the advantage over simple image differencing/thresholding, automated change detection algorithms, and postclassification techniques by characterizing press (gradual) and pulse (rapid) disturbances, providing spatially explicit estimates of uncertainty, and calibrating models using expert knowledge and a large dataset. As additional interpretations of change become available, the accuracy of change maps can be further assessed and models may be refined to account for change processes that may be underrepresented within the model training dataset. Current limitations include uncertainties of error propagation by various parameters, mapping issues associated with scale (e.g., mixed pixel effects), a paucity of Landsat data during the 1990s, and a lack of contemporaneously acquired ground-truth data. Future work may benefit by using techniques that explicitly account for autocorrelation and provide timing of disturbance information. However, recent work suggests that automated change detection algorithms typically need to be calibrated using training data and can be heavily impacted by noise (Cohen et al., 2017). Integration of vertical change data (e.g., Alonzo et al., 2017) would be beneficial for characterizing changes in ecosystem structure (due to thermokarst, e.g.,) that may not be apparent from optical imagery alone.

Despite these limitations, our results serve as a first step toward a comprehensive integration of diverse drivers and characterization of dramatic changes that have occurred across Alaska over the last 32 years. This comprehensive assessment of change drivers is unique in that it attributes changes observed in remotely sensed data to climatic, ecological, and geomorphological processes that have occurred throughout Alaska. By integrating observations of change processes with geospatial data and statistical models, we identified regional factors driving ecosystem dynamics and identify areas most vulnerable to change. According to our analysis, approximately 13% of Alaska has experienced change over the last three decades, with the majority of change occurring in boreal regions due to the residual effects of fires that are still apparent after 60 years. Our findings suggest that Landsat-based trend and change maps will be useful inputs for a suite of Earth System models; for example, by providing information that can constrain understanding of the trajectories, rates, and patterns of vegetation growth and succession. It is important to continue to detect land- and water-surface changes, and determine causation at a multitude of scales, to better understand how northern high-latitude ecosystems will respond to further perturbations and influence socio-ecological systems.

ORCID

Neal J. Pastick   http://orcid.org/0000-0002-4321-6739
Scott J. Goetz   http://orcid.org/0000-0002-6326-4308
Benjamin M. Jones   http://orcid.org/0000-0002-1517-4711
Bruce K. Wylie   http://orcid.org/0000-0002-7374-1083
Burke J. Minsley   http://orcid.org/0000-0003-1689-1306
Hélène Genet   http://orcid.org/0000-0003-4537-9563

REFERENCES

Abbott, B. W., Jones, J. B., Schuur, E. A. G., Chapin, F. S. III, Bowden, W. B., Bret-Harte, M. S., ... Zimov, S. (2016). Biomass offsets little or none of permafrost carbon release from soils, streams, and wildfire: An expert assessment. *Environmental Research Letters*, 11(3), 034014. https://doi.org/10.1088/1748-9326/11/3/034014

Ackerman, D., Griffin, D., Hobbie, S. E., & Finlay, J. C. (2017). Arctic shrub growth trajectories differ across soil moisture levels. *Global Change Biology*, 23(10), 4294–4302. https://doi.org/10.1111/gcb.13677

Alaback, P. B. (1982). Forest community structural change during secondary succession in southeast Alaska. In Proceedings of the Symposium: Forest Succession and Stand Development Research in the Northwest, 26 Mar. 1981, Corvallis, Oreg. Edited by J. E. Means. Oregon State University, Forestry Research Laboratory, Corvallis, Oreg. pp. 70–79.

Alexander, H. D., Mack, M. C., Goetz, S., Beck, P. S. A., & Belshe, E. F. (2012). Implications of increased deciduous cover on stand structure and aboveground carbon pools of Alaskan boreal forests. *Ecosphere*, 3(5), art45. https://doi.org/10.1890/ES11-00364.1

Alonzo, M., Morton, D. C., Cook, B. D., Andersen, H.-E., Babcock, C., & Pattison, R. (2017). Patterns of canopy and surface layer consumption in a boreal forest fire from repeat airborne lidar. *Environmental Research Letters*, 12(6), 065004. https://doi.org/10.1088/1748-9326/aa6ade

Arp, C. D., Jones, B. M., Schmutz, J. A., Urban, F. E., & Jorgenson, M. T. (2010). Two mechanisms of aquatic and terrestrial habitat change along an Alaskan Arctic coastline. *Polar Biology*, 33(12), 1629–1640. https://doi.org/10.1007/s00300-010-0800-5

Balser, A. W., Jones, J. B., & Gens, R. (2014). Timing of retrogressive thaw slump initiation in the Noatak Basin, northwest Alaska, USA. *Journal of Geophysical Research: Earth Surface*, 119(5), 1106–1120. https://doi.org/10.1002/2013JF002889

Beck, P. S. A., & Goetz, S. J. (2011). Satellite observations of high northern latitude vegetation productivity changes between 1982 and 2008: Ecological variability and regional differences. *Environmental Research Letters*, 6(4), 045501. https://doi.org/10.1088/1748-9326/6/4/045501

Beck, P. S. A., Goetz, S. J., Mack, M. C., Alexander, H. D., Jin, Y., Randerson, J. T., & Loranty, M. M. (2011). The impacts and implications of an intensifying fire regime on Alaskan boreal forest composition and albedo: Fire regime effects on boreal forests. *Global Change Biology*, 17(9), 2853–2866. https://doi.org/10.1111/j.1365-2486.2011.02412.x

Bentz, B., Régnière, J., Fettig, C., Hansen, E., Hayes, J., Hicke, J., & Seybold, S. (2010). Climate change and bark beetles of the western United States and Canada: Direct and indirect effects. *BioScience*, 60(8), 602–613. https://doi.org/10.1525/bio.2010.60.8.6

Berg, E. E., Henry, J. D., Fastie, C. L., De Volder, A. D., & Matsuoka, S. M. (2006). Spruce beetle outbreaks on the Kenai Peninsula, Alaska, and Kluane National Park and Reserve, Yukon Territory: Relationship to summer temperatures and regional differences in disturbance regimes. *Forest Ecology and Management*, 227(3), 219–232. https://doi.org/10.1016/j.foreco.2006.02.038

Berthier, E., Schiefer, E., Clarke, G. K. C., Menounos, B., & Rémy, F. (2010). Contribution of Alaskan glaciers to sea-level rise derived from satellite imagery. *Nature Geoscience*, 3(2), 92–95. https://doi.org/10.1038/ngeo737

Bond-Lamberty, B., Wang, C., & Gower, S. T. (2004). Net primary production and net ecosystem production of a boreal black spruce wildfire chronosequence. *Global Change Biology*, 10(4), 473–487. https://doi.org/10.1111/j.1529-8817.2003.0742.x

Bonfils, C. J. W., Phillips, T. J., Lawrence, D. M., Cameron-Smith, P., Riley, W. J., & Subin, Z. M. (2012). On the influence of shrub height and expansion on northern high latitude climate. *Environmental Research Letters*, 7(1), 015503. https://doi.org/10.1088/1748-9326/7/1/015503

Brown, L. E., & Milner, A. M. (2012). Rapid loss of glacial ice reveals stream community assembly processes. *Global Change Biology*, 18(7), 2195–2204. https://doi.org/10.1111/j.1365-2486.2012.02675.x

Brown, R. D., & Mote, P. W. (2009). The response of Northern Hemisphere snow cover to a changing climate. *Journal of Climate*, 22(8), 2124–2145. https://doi.org/10.1175/2008JCLI2665.1

Calef, M. P., Varvak, A., McGuire, A. D., Chapin, F. S., & Reinhold, K. B. (2015). Recent changes in annual area in interior Alaska: The impact of fire management. *Earth Interactions*, 19(5), 1–17. https://doi.org/10.1175/EI-D-14-0025.1

Carroll, M. L., Townshend, J. R. G., DiMiceli, C. M., Loboda, T., & Sohlberg, R. A. (2011). Shrinking lakes of the Arctic: Spatial relationships and trajectory of change: Shrinking lakes of the Arctic. *Geophysical Research Letters*, 38(20), 1–5. https://doi.org/10.1029/2011GL049427

Chapin, F. S. III, Eugster, W., McFadden, J. P., Lynch, A. H., & Walker, D. A. (2000). Summer differences among arctic ecosystems in regional climate forcing. *Journal of Climate*, 13(12), 2002–2010. https://doi.org/10.1175/1520-0442(2000)013<2002:SDAAEI>2.0.CO;2

Chapin, F. S., McGuire, A. D., Ruess, R. W., Hollingsworth, T. N., Mack, M. C., Johnstone, J. F., ... Taylor, D. L. (2010). Resilience of Alaska's boreal forest to climatic change. *Canadian Journal of Forest Research*, 40(7), 1360–1370. https://doi.org/10.1139/X10-074

Chapin, F. III, Robards, M., Huntington, H., Johnstone, J., Trainor, S., Kofinas, G., & Naylor, R. (2006). Directional changes in ecological communities and social-ecological systems: A framework for prediction based on Alaskan examples. *The American Naturalist*, 168(S6), S36–S49. https://doi.org/10.2307/4122279

Chapin, F. S., Walker, L. R., Fastie, C. L., & Sharman, L. C. (1994). Mechanisms of primary succession following deglaciation at Glacier Bay, Alaska. *Ecological Monographs*, 64(2), 149–175. https://doi.org/10.2307/2937039

Cohen, W., Healey, S., Yang, Z., Stehman, S., Brewer, C., Brooks, E., ... Zhu, Z. (2017). How similar are forest disturbance maps derived from different landsat time series algorithms? *Forests*, 8(4), 98. https://doi.org/10.3390/f8040098

Daly, C., Halbleib, M., Smith, J. I., Gibson, W. P., Doggett, M. K., Taylor, G. H., ... Pasteris, P. P. (2008). Physiographically sensitive mapping of climatological temperature and precipitation across the conterminous United States. *International Journal of Climatology*, 28(15), 2031–2064. https://doi.org/10.1002/joc.1688

Deal, R., & Farr, W. (1994). Composition and development of conifer regeneration in thinned and unthinned natural stands of western hemlock and Sitka spruce in southeast Alaska. *Canadian Journal of Forest Research*, 24(5), 976–984. https://doi.org/10.1139/x94-128

Dellasala, D. A., Hagar, J. C., Engel, K. A., McComb, W. C., Fairbanks, R. L., & Campbell, E. G. (1996). Effects of silvicultural modifications of temperate rainforest on breeding and wintering bird communities, Prince of Wales Island, Southeast Alaska. *The Condor*, 98(4), 706–721. https://doi.org/10.2307/1369853

Duffy, P., Walsh, J., Graham, J., Mann, D., & Rupp, T. (2005). Impacts of large-scale atmospheric–ocean variability on Alaskan fire season severity. *Ecological Applications*, 15(4), 1317–1330. https://doi.org/10.1890/04-0739

Duguay, C. R., Bernier, M., Gauthier, Y., & Kouraev, A. (2015). Remote sensing of lake and river ice. *Remote Sensing of the Cryosphere*. https://doi.org/10.1002/9781118368909.ch12

Eidenshink, J., Schwind, B., Brewer, K., Zhu, Z., Quayle, B., & Howard, S. (2007). A project for monitoring trends in burn severity. *Fire Ecology*, 3(1), 3–21. Fire Ecology Special Issue Vol, 3, 4. https://doi.org/10.4996/fireecology

Euskirchen, E. S., Bennett, A. P., Breen, A. L., Genet, H., Lindgren, M. A., Kurkowski, T. A., ... Rupp, T. S. (2016). Consequences of changes in

vegetation and snow cover for climate feedbacks in Alaska and northwest Canada. *Environmental Research Letters*, 11(10), 105003. https://doi.org/10.1088/1748-9326/11/10/105003

Fellman, J. B., Hood, E., Raymond, P. A., Hudson, J., Bozeman, M., & Arimitsu, M. (2015). Evidence for the assimilation of ancient glacier organic carbon in a proglacial stream food web: Assimilation of glacier organic carbon. *Limnology and Oceanography*, 60(4), 1118–1128. https://doi.org/10.1002/lno.10088

Fernandes, R., & Leblanc, S. G. (2005). Parametric (modified least squares) and non-parametric (Theil–Sen) linear regressions for predicting biophysical parameters in the presence of measurement errors. *Remote Sensing of Environment*, 95(3), 303–316. https://doi.org/10.1016/j.rse.2005.01.005

Flint, P., Mallek, L., King, E., Schmutz, J., Bollinger, R., & Derksen, J. (2008). Changes in abundance and spatial distribution of geese molting near Teshekpuk Lake, Alaska: Interspecific competition or ecological change? *Polar Biology*, 31(5), 549–556. https://doi.org/10.1007/s00300-007-0386-8

Fraser, R. H., Olthof, I., Carrière, M., Deschamps, A., & Pouliot, D. (2011). Detecting long-term changes to vegetation in northern Canada using the Landsat satellite image archive. *Environmental Research Letters*, 6(4), 045502. https://doi.org/10.1088/1748-9326/6/4/045502

Fraser, R. H., Olthof, I., Kokelj, S. V., Lantz, T. C., Lacelle, D., Brooker, A., ... Schwarz, S. (2014). Detecting landscape changes in high latitude environments using landsat trend analysis: 1. Visualization. *Remote Sensing*, 6(11), 11533–11557. https://doi.org/10.3390/rs61111533

Gallaun, H., Steinegger, M., Wack, R., Schardt, M., Kornberger, B., & Schmitt, U. (2015). Remote sensing based two-stage sampling for accuracy assessment and area estimation of land cover changes. *Remote Sensing*, 7(9), 11992–12008. https://doi.org/10.3390/rs70911992

Gao, B.-C. (1996). NDWI—A normalized difference water index for remote sensing of vegetation liquid water from space. *Remote Sensing of Environment*, 58(3), 257–266. https://doi.org/10.1016/S0034-4257(96)00067-3

Genet, H., He, Y., Lyu, Z., McGuire, A., Zhuang, Q., Clein, J., & Zhu, Z. (2018). The role of driving factors in historical and projected carbon dynamics of upland ecosystems in Alaska. *Ecological Applications*, 28(1), 5–27. https://doi.org/10.1002/eap.1641

Goetz, Scott J., Bunn, Andrew G., Fiske, Gregory J., & Houghton, R. A. (2005). Satellite-observed photosynthetic trends across boreal North America associated with climate and fire disturbance. *Proceedings of the National Academy of Sciences of the United States of America*, 102(38), 13521–13525. https://doi.org/10.1073/pnas.0506179102

Goetz, S. J., & Prince, S. D. (1999). Modeling terrestrial carbon exchange and storage: Evidence and implications of functional convergence in light use efficiency. *Advances in Ecological Research*, 28, 57–92. https://doi.org/10.1016/S0065-2504(08)60029-X

Gorelick, N., Hancher, M., Dixon, M., Ilyushchenko, S., Thau, D., & Moore, R. (2017). Google earth engine: Planetary-scale geospatial analysis for everyone. *Remote Sensing of Environment*, https://doi.org/10.1016/j.rse.2017.06.031

Gottfried, M., Pauli, H., Futschik, A., Akhalkatsi, M., Barančok, P., Benito Alonso, J. L., ... Grabherr, G. (2012). Continent-wide response of mountain vegetation to climate change. *Nature Climate Change*, 2(2), 111–115. https://doi.org/10.1038/nclimate1329

Hallet, B., Hunter, L., & Bogen, J. (1996). Rates of erosion and sediment evacuation by glaciers: A review of field data and their implications. *Global and Planetary Change*, 12(1–4), 213–235. https://doi.org/10.1016/0921-8181(95)00021-6

Hansen, M. C., Potapov, P. V., Moore, R., Hancher, M., Turubanova, S. A., Tyukavina, A., ... Townshend, J. R. G. (2013). High-resolution global maps of 21st-century forest cover change. *Science*, 342(6160), 850–853. https://doi.org/10.1126/science.1244693

Harris, I., Jones, P. D., Osborn, T. J., & Lister, D. H. (2014). Updated high-resolution grids of monthly climatic observations – the CRU TS3.10 dataset: updated high-resolution grids of monthly climatic observations. *International Journal of Climatology*, 34(3), 623–642. https://doi.org/10.1002/joc.3711

Hayes, D. J., Guo, L., & McGuire, A. D. (2007). A scientific synthesis and assessment of the Arctic carbon cycle. *Eos, Transactions American Geophysical Union*, 88(26), https://doi.org/10.1029/2007EO260007

Hayhoe, K., VanDorn, J., Croley, T., Schlegal, N., & Wuebbles, D. (2010). Regional climate change projections for Chicago and the US Great Lakes. *Journal of Great Lakes Research*, 36, 7–21. https://doi.org/10.1016/j.jglr.2010.03.012

Hermosilla, T., Wulder, M. A., White, J. C., Coops, N. C., & Hobart, G. W. (2015). Regional detection, characterization, and attribution of annual forest change from 1984 to 2012 using Landsat-derived time-series metrics. *Remote Sensing of Environment*, 170, 121–132. https://doi.org/10.1016/j.rse.2015.09.004

Hicke, J. A., Johnson, M. C., Hayes, J. L., & Preisler, H. K. (2012). Effects of bark beetle-caused tree mortality on wildfire. *Forest Ecology and Management*, 271, 81–90. https://doi.org/10.1016/j.foreco.2012.02.005

Hinkel, K. M., Jones, B. M., Eisner, W. R., Cuomo, C. J., Beck, R. A., & Frohn, R. (2007). Methods to assess natural and anthropogenic thaw lake drainage on the western Arctic coastal plain of northern Alaska. *Journal of Geophysical Research*, 112(F2), https://doi.org/10.1029/2006JF000584

Hinzman, L. D., Bettez, N. D., Bolton, W. R., Chapin, F. S., Dyurgerov, M. B., Fastie, C. L., ... Yoshikawa, K. (2005). Evidence and implications of recent climate change in northern Alaska and other Arctic regions. *Climatic Change*, 72(3), 251–298. https://doi.org/10.1007/s10584-005-5352-2

Hinzman, L., Deal, C., McGuire, A., Mernild, S., Polyakov, I., & Walsh, J. (2013). Trajectory of the Arctic as an integrated system. *Ecological Applications*, 23(8), 1837–1868. https://doi.org/10.1890/11-1498.1

Holden, C. E., & Woodcock, C. E. (2016). An analysis of Landsat 7 and Landsat 8 underflight data and the implications for time series investigations. *Remote Sensing of Environment*, 185, 16–36. https://doi.org/10.1016/j.rse.2016.02.052

Houseknecht, D., & Bird, K., & Geological Survey (2006). *Oil and gas resources of the Arctic Alaska petroleum province*. U.S. Geological Survey Professional Paper 1732-A, 1–11. Retrieved from http://pubs.usgs.gov/pp/pp1732a/

Huss, M., Bookhagen, B., Huggel, C., Jacobsen, D., Bradley, R. S., Clague, J. J., ... Winder, M. (2017). Toward mountains without permanent snow and ice: Mountains without permanent snow and ice. *Earth's Future*, https://doi.org/10.1002/2016EF000514

Jepsen, S. M., Walvoord, M. A., Voss, C. I., & Rover, J. (2016). Effect of permafrost thaw on the dynamics of lakes recharged by ice-jam floods: Case study of Yukon Flats, Alaska: Effect of permafrost thaw on the dynamics of flood-recharged lakes. *Hydrological Processes*, 30(11), 1782–1795. https://doi.org/10.1002/hyp.10756

Ji, L., Wylie, B. K., Nossov, D. R., Peterson, B., Waldrop, M. P., McFarland, J. W., ... Hollingsworth, T. N. (2012). Estimating aboveground biomass in interior Alaska with Landsat data and field measurements. *International Journal of Applied Earth Observation and Geoinformation*, 18, 451–461. https://doi.org/10.1016/j.jag.2012.03.019

Johnstone, J. F., Hollingsworth, T. N., Chapin, F. S., & Mack, M. C. (2010). Changes in fire regime break the legacy lock on successional trajectories in Alaskan boreal forest. *Global Change Biology*, 16(4), 1281–1295. https://doi.org/10.1111/j.1365-2486.2009.02051.x

Johnstone, J., Rupp, F., Olson, T., & Verbyla, S. (2011). Modeling impacts of fire severity on successional trajectories and future fire behavior in Alaskan boreal forests. *Landscape Ecology*, 26(4), 487–500. https://doi.org/10.1007/s10980-011-9574-6

Jones, B. M. (2008). Land-cover change on the southern Kenai Peninsula lowlands, Alaska using USGS land cover trends. *Journal of Geography and Regional Planning*, 1(4), 68–71.

Jones, B. M., Arp, C. D., Jorgenson, M. T., Hinkel, K. M., Schmutz, J. A., & Flint, P. L. (2009). Increase in the rate and uniformity of coastline erosion in Arctic Alaska. *Geophysical Research Letters*, *36*(3), 1–5. https://doi.org/10.1029/2008GL036205

Jones, Benjamin M., Baughman, Carson A., Romanovsky, Vladimir E., Parsekian, Andrew D., Babcock, Esther L., Stephani, Eva, & Berg, Edward E. (2016). Presence of rapidly degrading permafrost plateaus in south-central Alaska. *The Cryosphere*, *10*(6), 2673–2692. https://doi.org/10.5194/tc-10-2673-2016

Jones, B. M., Grosse, G., Arp, C. D., Jones, M. C., Walter Anthony, K. M., & Romanovsky, V. E. (2011). Modern thermokarst lake dynamics in the continuous permafrost zone, northern Seward Peninsula, Alaska. *Journal of Geophysical Research: Biogeosciences*, *116*(G2), 1–3. https://doi.org/10.1029/2011JG001666

Jones, B. M., Grosse, G., Arp, C. D., Miller, E., Liu, L., Hayes, D. J., & Larsen, C. F. (2015). Recent Arctic tundra fire initiates widespread thermokarst development. *Scientific Reports*, *5*, 15865. https://doi.org/10.1038/srep15865

Jones, B. M., Hinkel, K. M., Arp, C. D., & Eisner, W. R. (2008). Modern erosion rates and loss of coastal features and sites, Beaufort Sea coastline, Alaska. *Arctic*, *61*(4), 361–372. https://doi.org/10.14430/Arctic44

Jorgenson, M. T., & Brown, J. (2005). Classification of the Alaskan Beaufort Sea Coast and estimation of carbon and sediment inputs from coastal erosion. *Geo-Marine Letters*, *25*(2–3), 69–80. https://doi.org/10.1007/s00367-004-0188-8

Jorgenson, M. T., & Brown, D. R. N. (2015). Patterns and rates of landscape change in central Alaska. In T. Douglas (Ed.), *Addressing the impacts of climate change on U.S. Army Alaska with decision support tools developed through field work and modeling* (pp. 45–63), *SERDP Fin. Rep.* Fairbanks, AK: U.S. Army Cold Regions Research and Engineering.

Jorgenson, M. T., Marcot, B. G., Swanson, D. K., Jorgenson, J. C., & DeGange, A. R. (2015). Projected changes in diverse ecosystems from climate warming and biophysical drivers in northwest Alaska. *Climatic Change*, *130*(2), 131–144. https://doi.org/10.1007/s10584-014-1302-1

Jorgenson, M. T., & Osterkamp, T. E. (2005). Response of boreal ecosystems to varying modes of permafrost degradation. *Canadian Journal of Forest Research*, *35*(9), 2100–2111. https://doi.org/10.1139/x05-153

Jorgenson, M. T., Racine, C., Walters, J., & Osterkamp, T. (2001). Permafrost degradation and ecological changes associated with a warming climate in central Alaska. *Climatic Change*, *48*(4), 551–579. https://doi.org/10.1023/A:1005667424292

Jorgenson, M. T., Shur, Y. L., & Pullman, E. R. (2006). Abrupt increase in permafrost degradation in Arctic Alaska. *Geophysical Research Letters*, *33*, 4. https://doi.org/10.1029/2005GL024960

Jorgenson, T., Yoshikawa, K., Kanevskiy, M., Shur, Y., Romanovsky, V., Marchenko, S., . . . Jones, B. (2008). Permafrost characteristics of Alaska–A new permafrost map of Alaska, in: Ninth International Conference on Permafrost. Presented at the Ninth International Conference on Permafrost, pp. 121–122.

Ju, J., & Masek, J. G. (2016). The vegetation greenness trend in Canada and US Alaska from 1984–2012 Landsat data. *Remote Sensing of Environment*, *176*, 1–16. https://doi.org/10.1016/j.rse.2016.01.001

Karlsson, J. M., Jaramillo, F., & Destouni, G. (2015). Hydro-climatic and lake change patterns in Arctic permafrost and non-permafrost areas. *Journal of Hydrology*, *529*, 134–145. https://doi.org/10.1016/j.jhydrol.2015.07.005

Karlsson, J. M., Lyon, S. W., & Destouni, G. (2012). Thermokarst lake, hydrological flow and water balance indicators of permafrost change in Western Siberia. *Journal of Hydrology*, *464–465*, 459–466. https://doi.org/10.1016/j.jhydrol.2012.07.037

Kasischke, E. S., & French, N. H. F. (1997). Constraints on using AVHRR composite index imagery to study patterns of vegetation cover in boreal forests. *International Journal of Remote Sensing*, *18*(11), 2403–2426. https://doi.org/10.1080/014311697217684

Kasischke, E. S., Verbyla, D. L., Rupp, T. S., McGuire, A. D., Murphy, K. A., Jandt, R., . . . Turetsky, M. R. (2010). Alaska's changing fire regime —implications for the vulnerability of its boreal forests. *Canadian Journal of Forest Research*, *40*(7), 1313–1324. https://doi.org/10.1139/X10-098

Klaar, M. J., Kidd, C., Malone, E., Bartlett, R., Pinay, G., Chapin, F. S., & Milner, A. (2015). Vegetation succession in deglaciated landscapes: Implications for sediment and landscape stability: Vegetation succession: Implications for sediment & landscape stability. *Earth Surface Processes and Landforms*, *40*(8), 1088–1100. https://doi.org/10.1002/esp.3691

Klein, E., Berg, E. E., & Dial, R. (2005). Wetland drying and succession across the Kenai Peninsula Lowlands, south-central Alaska. *Canadian Journal of Forest Research*, *35*(8), 1931–1941. https://doi.org/10.1139/x05-129

Lantz, T. C., Kokelj, S. V., Gergel, S. E., & Henry, G. H. R. (2009). Relative impacts of disturbance and temperature: Persistent changes in microenvironment and vegetation in retrogressive thaw slumps. *Global Change Biology*, *15*(7), 1664–1675. https://doi.org/10.1111/j.1365-2486.2009.01917.x

Lara, M. J., Genet, H., McGuire, A. D., Euskirchen, E. S., Zhang, Y., Brown, D. R. N., . . . Bolton, W. R. (2016). Thermokarst rates intensify due to climate change and forest fragmentation in an Alaskan boreal forest lowland. *Global Change Biology*, *22*(2), 816–829. https://doi.org/10.1111/gcb.13124

Larsen, C. F., Burgess, E., Arendt, A. A., O'Neel, S., Johnson, A. J., & Kienholz, C. (2015). Surface melt dominates Alaska glacier mass balance: Alaska glacier mass balance. *Geophysical Research Letters*, *42*(14), 5902–5908. https://doi.org/10.1002/2015GL064349

Larsen, C. F., Motyka, R. J., Arendt, A. A., Echelmeyer, K. A., & Geissler, P. E. (2007). Glacier changes in southeast Alaska and northwest British Columbia and contribution to sea level rise. *Journal of Geophysical Research*, *112*(F1), https://doi.org/10.1029/2006JF000586

Lawrence, D. M., & Swenson, S. C. (2011). Permafrost response to increasing Arctic shrub abundance depends on the relative influence of shrubs on local soil cooling versus large-scale climate warming. *Environmental Research Letters*, *6*(4), 045504. https://doi.org/10.1088/1748-9326/6/4/045504

Loranty, M., & Goetz, S. (2012). Shrub expansion and climate feedbacks in Arctic tundra. *Environmental Research Letters*, *7*(1), 1–3.

Loranty, M., Lieberman-Cribbin, W., Berner, L., Natali, S., Goetz, S., Alexander, H., & Kholodov, A. (2016). Spatial variation in vegetation productivity trends, fire disturbance, and soil carbon across Arctic-boreal permafrost ecosystems. *Environmental Research Letters*, *11*(9), 13.

Loso, M., Arendt, A., Larsen, C., Rich, J., & Murphy, N. (2014). Alaskan national park glaciers – status and trends: Final report. Natural Resource Technical Report NPS/AKRO/NRTR—2014/922. National Park Service, Fort Collins, Colorado.

Malmström, C. M., & Raffa, K. F. (2000). Biotic disturbance agents in the boreal forest: Considerations for vegetation change models. *Global Change Biology*, *6*(S1), 35–48. https://doi.org/10.1046/j.1365-2486.2000.06012.x

Margolis, H. A., Nelson, R. F., Montesano, P. M., Beaudoin, A., Sun, G., Andersen, H.-E., & Wulder, M. A. (2015). Combining satellite lidar, airborne lidar, and ground plots to estimate the amount and distribution of aboveground biomass in the boreal forest of North America 1. *Canadian Journal of Forest Research*, *45*(7), 838–855. https://doi.org/10.1139/cjfr-2015-0006

Markham, B. L., & Helder, D. L. (2012). Forty-year calibrated record of earth-reflected radiance from Landsat: A review. *Remote Sensing of Environment*, *122*, 30–40. https://doi.org/10.1016/j.rse.2011.06.026

McGrath, D., Sass, L., O'Neel, S., Arendt, A., & Kienholz, C. (2017). Hypsometric control on glacier mass balance sensitivity in Alaska and northwest Canada. *Earth's Future*, 5(3), 324–336. https://doi.org/10.1002/2016EF000479

Myers-Smith, I. H., Forbes, B. C., Wilmking, M., Hallinger, M., Lantz, T., Blok, D., . . . Hik, D. S. (2011). Shrub expansion in tundra ecosystems: Dynamics, impacts and research priorities. *Environmental Research Letters*, 6(4), 045509. https://doi.org/10.1088/1748-9326/6/4/045509

Nitze, I., Grosse, G., Jones, B., Arp, C., Ulrich, M., Fedorov, A., & Veremeeva, A. (2017). Landsat-based trend analysis of lake dynamics across northern permafrost regions. *Remote Sensing*, 9(7), https://doi.org/10.3390/rs9070640

Nowacki, G., Spencer, P., Fleming, M., Brock, T., & Jorgenson, M.T. (2003). Unified ecoregions of Alaska; 2001: U.S. Geological survey open-file report 02–297, 1 map.

Olofsson, P., Foody, G. M., Herold, M., Stehman, S. V., Woodcock, C. E., & Wulder, M. A. (2014). Good practices for estimating area and assessing accuracy of land change. *Remote Sensing of Environment*, 148, 42–57. https://doi.org/10.1016/j.rse.2014.02.015

Olthof, I., & Fraser, H. R. (2014). Detecting landscape changes in high latitude environments using landsat trend analysis: 2. Classification. *Remote Sensing*, 6(11), 11558–11578. https://doi.org/10.3390/rs61111558

Parent, M. B., & Verbyla, D. (2010). The browning of Alaska's boreal forest. *Remote Sensing*, 2(12), 2729–2747. https://doi.org/10.3390/rs2122729

Pastick, N. J., Duffy, P., Genet, H., Rupp, T. S., Wylie, B. K., Johnson, K. D., . . . Jafarov, E. E. (2017). Historical and projected trends in landscape drivers affecting carbon dynamics in Alaska. *Ecological Applications*, 27(5), 1383–1402. https://doi.org/10.1002/eap.1538

Pastick, N. J., Jorgenson, M. T., Goetz, S. J., Jones, B. M., Wylie, B. K., Minsley, B. J., . . . Jorgenson, J. C. (2018). Probabilistic estimates of landscape change in Alaska (1984 to 2015): U.S. Geological Survey data release, https://doi.org/10.5066/f7dv1j6n

Pastick, N. J., Jorgenson, M. T., Wylie, B. K., Nield, S. J., Johnson, K. D., & Finley, A. O. (2015). Distribution of near-surface permafrost in Alaska: Estimates of present and future conditions. *Remote Sensing of Environment*, 168, 301–315. https://doi.org/10.1016/j.rse.2015.07.019

Pearson, R. G., Phillips, S. J., Loranty, M. M., Beck, P. S. A., Damoulas, T., Knight, S. J., & Goetz, S. J. (2013). Shifts in Arctic vegetation and associated feedbacks under climate change. *Nature Climate Change*, 3(7), 673–677. https://doi.org/10.1038/nclimate1858

Pekel, J.-F., Cottam, A., Gorelick, N., & Belward, A. S. (2016). High-resolution mapping of global surface water and its long-term changes. *Nature*, 540(7633), 418–422. https://doi.org/10.1038/nature20584

Pickett, S. T. A. (1989). Space-for-time substitution as an alternative to long-term studies. In G. E. Likens (Ed.), *Long-term studies in ecology: Approaches and alternatives*. New York, NY: Springer-Verlag.

Quinlan, J. R. (1986). Induction of decision trees. *Machine Learning*, 1(1), 81–106.

Quinlan, J. R. (1993). *C4.5: Programs for machine learning*. San Francisco, CA: Morgan Kaufmann Publishers.

R Core Team. (2015). *R: A language and environment for statistical computing*. Vienna, Austria: R Foundation for Statistical Computing. Retrieved from http://www.R-project.org/

Raynolds, M. K., & Walker, D. A. (2016). Increased wetness confounds Landsat-derived NDVI trends in the central Alaska North slope region, 1985–2011. *Environmental Research Letters*, 11(8), 085004. https://doi.org/10.1088/1748-9326/11/8/085004

Riley, S. J., DeGloria, S. D., & Elliot, R. (1999). A terrain ruggedness index that quantifies topographic heterogeneity. *Intermountain Journal of Sciences*, 5(1–4), 1999.

Roach, J. K., Griffith, B., & Verbyla, D. (2013). Landscape influences on climate-related lake shrinkage at high latitudes. *Global Change Biology*, 19(7), 2276–2284. https://doi.org/10.1111/gcb.12196

Roach, J., Griffith, B., Verbyla, D., & Jones, J. (2011). Mechanisms influencing changes in lake area in Alaskan boreal forest: Mechanisms for lake area change in ALASKA. *Global Change Biology*, 17(8), 2567–2583. https://doi.org/10.1111/j.1365-2486.2011.02446.x

Robson, B. A., Nuth, C., Dahl, S. O., Hölbling, D., Strozzi, T., & Nielsen, P. R. (2015). Automated classification of debris-covered glaciers combining optical, SAR and topographic data in an object-based environment. *Remote Sensing of Environment*, 170, 372–387. https://doi.org/10.1016/j.rse.2015.10.001

Rocha, A., Loranty, M., Higuera, P., Mack, M., Hu, F., Jones, B., & Shaver, G. (2012). The footprint of Alaskan tundra fires during the past half-century: Implications for surface properties and radiative forcing. *Environmental Research Letters*, 7(4), 8.

Rogers, B. M., Randerson, J. T., & Bonan, G. B. (2013). High latitude cooling associated with landscape changes from North American boreal forest fires. *Biogeosciences*, 10, 699–718. https://doi.org/10.5194/bg-10-699-2013

Rogers, B. M., Solvik, K., Hogg, E. H., Ju, J., Masek, J. G., Michaelian, M., . . . Goetz, S. J. (2018). Detecting early warning signals of tree mortality in boreal North America using multi-scale satellite data. *Global Change Biology*, 1–21. https://doi.org/10.1111/gcb.14107

Romme, W., Knight, D., & Yavitt, J. (1986). Mountain pine beetle outbreaks in the Rocky Mountains: Regulators of primary productivity. *The American Naturalist*, 127(4), 484–494. https://doi.org/10.1086/284497

Roy, D. P., Kovalskyy, V., Zhang, H. K., Vermote, E. F., Yan, L., Kumar, S. S., & Egorov, A. (2016). Characterization of Landsat-7 to Landsat-8 reflective wavelength and normalized difference vegetation index continuity. *Remote Sensing of Environment*, 185, 57–70. https://doi.org/10.1016/j.rse.2015.12.024

Sigman, M. (1985). *Impacts of clearcut logging on the fish and wildlife resources of southeast, Alaska*. Juneau, AK: Alaska Dept. of Fish and Game, Habitat Division.

Smith, L. C., Sheng, Y., & MacDonald, G. M. (2007). A first pan-Arctic assessment of the influence of glaciation, permafrost, topography and peatlands on northern hemisphere lake distribution. *Permafrost and Periglacial Processes*, 18(2), 201–208. https://doi.org/10.1002/ppp.581

Soja, A. J., Tchebakova, N. M., French, N. H. F., Flannigan, M. D., Shugart, H. H., Stocks, B. J., . . . Stackhouse, P. W. (2007). Climate-induced boreal forest change: Predictions versus current observations. *Global and Planetary Change*, 56(3), 274–296. https://doi.org/10.1016/j.gloplacha.2006.07.028

Sommaruga, R. (2015). When glaciers and ice sheets melt: Consequences for planktonic organisms. *Journal of Plankton Research*, 37(3), 509–518. https://doi.org/10.1093/plankt/fbv027

Steele, M., Ermold, W., & Zhang, J. (2008). Arctic Ocean surface warming trends over the past 100 years. *Geophysical Research Letters*, 35(2), 1–6. https://doi.org/10.1029/2007GL031651

Stroeve, J., Serreze, M., Drobot, S., Gearheard, S., Holland, M., Maslanik, J., . . . Scambos, T. (2008). Arctic sea ice extent plummets in 2007. *Eos, Transactions American Geophysical Union*, 89(2), https://doi.org/10.1029/2008EO020001

Sturm, M., Douglas, T., Racine, C., & Liston, G. (2005). Changing snow and shrub conditions affect albedo with global implications. *Journal of Geophysical Research: Biogeosciences*, 110(G1), https://doi.org/10.1029/2005JG000013

Swanson, D. K. (2013). Three decades of landscape change in Alaska's Arctic National Parks: Analysis of aerial photographs, c. 1980-2010. Natural Resource Technical Report NPS/ARCN/NRTR—2013/668. National Park Service, Fort Collins, CO.

Swanson, D. K. (2014). Mapping of erosion features related to thaw of permafrost in the NPS Arctic Inventory and Monitoring Network, Alaska. Natural Resource Technical Report NPS/ARCN/NRTR—2014/912. National Park Service, Fort Collins, Colorado.

Tape, K. D., Flint, P. L., Meixell, B. W., & Gaglioti, B. V. (2013). Inundation, sedimentation, and subsidence creates goose habitat along the Arctic coast of Alaska. *Environmental Research Letters*, 8(4), 045031. https://doi.org/10.1088/1748-9326/8/4/045031

Trugman, A. T., Medvigy, D., Anderegg, W. R. L., & Pacala, S. W. (2018). Differential declines in Alaskan boreal forest vitality related to climate and competition. *Global Change Biology*, 24, 1097–1107. https://doi.org/10.1111/gcb.13952

Verbyla, D. (2011). Browning boreal forests of western North America. *Environmental Research Letters*, 6(4), 041003. https://doi.org/10.1088/1748-9326/6/4/041003

Walker, D. A., Leibman, M. O., Epstein, H. E., Forbes, B. C., Bhatt, U. S., Raynolds, M. K., … Yu, Q. (2009). Spatial and temporal patterns of greenness on the Yamal Peninsula, Russia: Interactions of ecological and social factors affecting the Arctic normalized difference vegetation index. *Environmental Research Letters*, 4(4), 045004. https://doi.org/10.1088/1748-9326/4/4/045004

Walvoord, M. A., Voss, C. I., & Wellman, T. P. (2012). Influence of permafrost distribution on groundwater flow in the context of climate-driven permafrost thaw: Example from Yukon Flats Basin, Alaska, United States. *Water Resources Research*, 48(7), W07524. https://doi.org/10.1029/2011WR011595

Winsvold, S. H., Kaab, A., & Nuth, C. (2016). Regional glacier mapping using optical satellite data time series. *IEEE Journal of Selected Topics in Applied Earth Observations and Remote Sensing*, 9(8), 3698–3711. https://doi.org/10.1109/JSTARS.2016.2527063

Wood, S. N. (2006). *Generalized additive models: An introduction with R.* Boca Raton, FL: CRC Press.

Yoshikawa, K., & Hinzman, L. D. (2003). Shrinking thermokarst ponds and groundwater dynamics in discontinuous permafrost near Council, Alaska. *Permafrost and Periglacial Processes*, 14(2), 151–160. https://doi.org/10.1002/(ISSN)1099-1530

Zhang, W., Miller, P. A., Smith, B., Wania, R., Koenigk, T., & Döscher, R. (2013). Tundra shrubification and tree-line advance amplify arctic climate warming: Results from an individual-based dynamic vegetation model. *Environmental Research Letters*, 8(3), 034023. https://doi.org/10.1088/1748-9326/8/3/034023

Zhou, X., Schroder, S. A., McGuire, A. D., & Zhu, Z. (2016). Forest inventory-based analysis and projections of forest carbon stocks and changes in Alaskan coastal forests. In Z. Zhu & A. D. McGuire (Eds.), *Baseline and projected future carbon storage and greenhouse-gas fluxes in ecosystems of Alaska* (pp. 95–104), US Geological Surey Professional Paper 1826, Reston, VA.

Zhu, Z., & Woodcock, C. E. (2014). Automated cloud, cloud shadow, and snow detection in multitemporal Landsat data: An algorithm designed specifically for monitoring land cover change. *Remote Sensing of the Environment*, 152, 217–234. https://doi.org/10.1016/j.rse.2014.06.012

SUPPORTING INFORMATION

Additional supporting information may be found online in the Supporting Information section at the end of the article.